Strain rate controlled compaction characterization of e-glass fabrics and investigation of the effects of process parameters on the results

by

Mustafa Reşit HABOĞLU

A Thesis Submitted to the

Graduate School of Engineering

in Partial Fulfillment of the Requirements for

the Degree of

Master of Science

in

Mechanical Engineering

Koc University

August 2012

Koc University

Graduate School of Sciences and Engineering

This is to certify that I have examined this copy of a master's thesis by

Mustafa Reşit Haboğlu

and have found that it is complete and satisfactory in all respects,
and that any and all revisions required by the final
examining committee have been made.

Committee Members:

_____

E. Murat Sözer, Ph. D. (Advisor)

_____

B. Erdem Alaca, Ph. D.

_____

Rıza Kızılel, Ph. D.

Date: _____

ABSTRACT

Strain rate controlled compaction/decompaction experiments were performed on various e-glass fabric preforms by using a conventional Vacuum Infusion (VI) experimental setup integrated with a laser displacement measurement sensor. A PID controller was designed to control the strain, and the stress was measured in an actual VI setup. Compared to the available characterization procedures in the literature, this approach allows investigating effects of different phenomena (such as dry to wet transition; rate of loading/unloading; and fabric settling/relaxation at major/minor loading) and mimicking the fabric compaction as in the actual VI setup itself instead of using a separate characterization setup. The experimental data is fitted with a compaction model to investigate the elastic and viscous components of a viscoelastic compaction model. The database constructed in this study will be useful for the comparison of pressure and strain rate controlled compaction characterization experiments; and decide on which approach is more appropriate to represent the fiber compaction in VI.

ÖZETÇE

Farklı cam elyaf tipleri üzerinde lazerle mesafe ölçüm sensörüne sahip bir Vakum İnfüzyon (VI) deneysel düzeneği üzerinde gerinim değişim hızı kontrol edilerek sıkıştırma/salma deneyleri gerçekleştirildi. Gerçek bir VI düzeneği üzerinde bir PID kontrol sistemi tasarlanarak gerinim kontrol edildi ve basınç ölçümü yapıldı. Bu yaklaşım, literatürde yer alan karakterizasyon prosedürlerine kıyasla, farklı olayların (örneğin numunenin kuruyken ıslak hale geçmesi; yükleme/boşaltma hızı; yüklemedeki üst/alt basınç limitleri; ve elyaf yerleşmesi/gevşemesi) incelenmesine ve farklı bir karakterizasyon düzeneğindense bir VI düzeneği kullanarak gerçek imalat usulünün taklit edilmesine olanak sağlar. Deneysel veriler bir viskoelastik sıkıştırma modelinin elastik ve akışkanlık unsurlarını incelemek için bir sıkıştırma modeline oturtuldu. Bu araştırmada oluşturulan veri tabanı, basınç veya gerinim değişim hızları kontrol edilerek yapılan sıkıştırma karakterizasyon deneylerinin karşılaştırılmasında ve hangi deney metodunun gerçek bir VI uygulamasındaki elyaf sıkıştırmasını temsil etmede daha uygun olduğuna karar vermekte kullanışlı bir araç olacaktır.

ACKNOWLEDGEMENTS

I would like to thank my advisor Murat Sözer for his help and support in my studies. His guidance during the study of this thesis played a very major role for the completion of it. I will always appreciate that he was always more than a teacher to me.

I would also like to thank Assoc. Prof. Erdem Alaca and Dr. Rıza Kızılel for their participation in this thesis committee.

I also want to thank my colleague, Bekir Yenilmez for his remarkable help and collaboration in working on this thesis, and Mert Hancıoğlu for his help on performing the experiments.

I gratefully thank to my lab-partners, Talha Akyol, Barış Çağlar, Mehmet Akif Yalçınkaya and Ayşen Sarıoğlu for creating such a wonderful working environment.

I also thank to Arda Aytekin, Mehmet Ayyıldız, Utku Boz, Berkay Gümüş and Mine Toker for sharing the joyful moments at Koc University.

I would like to express my sincere thanks to Berkay Yarpuzlu, Nazire Bodancı, Uğur Yazıcı, Houman Zarsazegar and Soner Somuncu for being there for me every time I needed.

Finally, I would like to dedicate this thesis to my parents Mehmet Galip Haboğlu and Mücella Haboğlu without whom I would achieve nothing. I keep the biggest thanks to them for their endless support and belief without any expectations.

TABLE OF CONTENTS

List of Tables vi

List of Figures vii

Nomenclature xi

Chapter 1: Introduction 1

1.1 Vacuum Infusion (VI) Process 1
1.2 Variation of Part Thickness (both spatially and with Time) during VI Process 1
1.3 Compaction Characterization Experiments in the Literature 3
1.4 Objective 7

Chapter 2: Experimental Setup and Procedure 8

2.1 Experimental Setup 8
2.1.1 PID Tuning of Pressure Rate Controlled Experiments 17
2.1.2 PID Tuning of Strain Rate Controlled Experiments 20
2.2 Fabrics 23
2.3 Test Fluid 24
2.4 Experimental Procedure 24
2.4.1 Pre-Experimental Procedure 24
2.4.2 Pressure Rate Controlled Experiments 25
2.4.3 Strain Rate Controlled Experiments 29

Chapter 3: Experimental Results **32**

Chapter 4: Model Fitting **55**

Chapter 5: Summary and Conclusion **74**

Bibliography **76**

Vita **79**

LIST OF TABLES

Table 2.1: Effects of increasing the PID constants on system response ……. 17

Table 2.2: Weights and superficial densities of the specimens used in the experiments 24

Table 3.1: The list of figures showing experimental results for random fabric with different experimental procedures such as varying dε/dt and $P_{relaxation}$ values, and wetting condition …… 32

Table 3.2: The list of figures showing experimental results for woven fabric with different experimental procedures such as varying dε/dt and $P_{relaxation}$ values, and wetting condition …… 33

Table 4.1: The list of figures showing model fits on experimental results for random fabric with different experimental procedures such as varying dε/dt and $P_{relaxation}$ values, and wetting condition …… 58

Table 4.2: The list of figures showing model fits on experimental results for woven fabric with different experimental procedures such as varying dε/dt and $P_{relaxation}$ values, and wetting condition …… 58

LIST OF FIGURES

Figure 2.1 Schematic of the experimental setup …… 9

Figure 2.2 Acrylic resin distributor assembled on the steel plate ……..... 10

Figure 2.3 Illustration of wetting of the specimen ……..... 11

Figure 2.4(a) Specimen placed on the experimental setup (top view) ……... 12

Figure 2.4(b) Specimen placed on the experimental setup (side view) ……..... 13

Figure 2.4(c) Specimen placed on the experimental setup (photograph) ……..... 13

Figure 2.5 Block diagram of PID control system for pressure rate controlled experiments ……..…… 15

Figure 2.6 Block diagram of PID control system for strain rate controlled experiments ... ……..…… 16

Figure 2.7 PID manual tuning for pressure rate controlled experiments (system behavior for different PID constants) ……..…. 19

Figure 2.8 PID manual tuning for strain rate controlled experiments (system behavior for different PID constants) ……..…… 22

Figure 2.9 E-glass fabrics used in the experiments ……... 23

Figure 2.10 Placement of the fabric and vacuum bag during the preparation of the experiment ……..…….……..… 25

Figure 2.11 : Pressure rate controlled characterization experiments by varying $P_{relaxation}$. 27

Figure 2.12 Pressure rate controlled characterization experiments by varying dP/dt ….. 28

Figure 2.13 Strain rate controlled characterization experiments by varying $P_{relaxation}$ …. 29

Figure 2.14 Strain rate controlled characterization experiments by varying dε/dt …….. 31

Figure 3.1 Experimental results for 8R; dε/dt=0.01 s^{-1}; $P_{relaxation}$=1 kPa; no wetting 34

Figure 3.2 Experimental results for 8R; dε/dt=0.01 s^{-1}; $P_{relaxation}$=1 kPa ……..... 35

Figure 3.3 Experimental results for 8R; dε/dt=0.02 s^{-1}; $P_{relaxation}$=1 kPa ……..... 36

Figure 3.4 Experimental results for 8R; dε/dt=0.005 s^{-1}; $P_{relaxation}$=1 kPa ……..... 37

Figure 3.5 Experimental results for 8R; dε/dt=0.01 s^{-1}; $P_{relaxation}$=5 kPa ……..... 38

Figure 3.6 Experimental results for 8R; dε/dt=0.01 s^{-1}; $P_{relaxation}$=10 kPa ……..... 39

Figure 3.7 Experimental results for 8R; dε/dt=0.01 s^{-1}; $P_{relaxation}$=40 kPa ……..... 40

Figure 3.8 Experimental results for 8W; dε/dt=0.01 s^{-1}; $P_{relaxation}$=1 kPa; no wetting ... 41

Figure 3.9 Experimental results for 8W; dε/dt=0.01 s^{-1}; $P_{relaxation}$=1 kPa …...……..... 42

Figure 3.10 Experimental results for 8W; dε/dt=0.02 s^{-1}; $P_{relaxation}$=1 kPa ……..…..... 43

Figure 3.11 Experimental results for 8W; dε/dt=0.005 s^{-1}; $P_{relaxation}$=1 kPa ……..... 44

Figure 3.12 Experimental results for 8W; dε/dt=0.01 s^{-1}; $P_{relaxation}$=5 kPa ……..... 45

Figure 3.13 Experimental results for 8W; dε/dt=0.01 s^{-1}; $P_{relaxation}$=10 kPa ……..…..... 46

Figure 3.14 Experimental results for 8W; dε/dt=0.01 s^{-1}; $P_{relaxation}$=40 kPa ……..... 47

Figure 3.15 The filtered and the raw strain data of experiment 1 for random fabric under nominal characterization parameters …… 49

Figure 3.16 The filtered and the raw thickness data of Experiment 1 for random fabric under nominal characterization parameters …….. 50

Figure 3.17 Case A (a = 2; b = 0.5): The filtered and the raw pressure data of experiment 1 for random fabric under nominal characterization parameters ……. 52

Figure 3.18 Case B (a = 2; b = 0.01): The filtered and the raw pressure data of experiment 1 for random fabric under nominal characterization parameters ……..… 53

Figure 3.19 Case C (using the "smooth" function): The filtered and the raw pressure data of experiment 1 for random fabric under nominal characterization parameters ……...… 54

Figure 4.1 Schematic of the mathematical model …….. 55

Figure 4.2 Model fits on experimental results for 8R; $d\varepsilon/dt=0.01\ s^{-1}$; $P_{relaxation}$=1 kPa; no wetting …….……. 59

Figure 4.3 Model fits on experimental results for 8R; $d\varepsilon/dt=0.01\ s^{-1}$; $P_{relaxation}$=1 kPa .. 60

Figure 4.4 Model fits on experimental results for 8R; $d\varepsilon/dt=0.02\ s^{-1}$; $P_{relaxation}$=1 kPa .. 61

Figure 4.5 Model fits on experimental results for 8R; $d\varepsilon/dt=0.005\ s^{-1}$; $P_{relaxation}$=1 kPa..62

Figure 4.6 Model fits on experimental results for 8R; $d\varepsilon/dt=0.01\ s^{-1}$; $P_{relaxation}$=5 kPa .. 63

Figure 4.7 Model fits on experimental results for 8R; $d\varepsilon/dt=0.01\ s^{-1}$; $P_{relaxation}$=10 kPa..64

Figure 4.8 Model fits on experimental results for 8R; $d\varepsilon/dt=0.01\ s^{-1}$; $P_{relaxation}$=40 kPa..65

Figure 4.9 Model fits on experimental results for 8R; $d\varepsilon/dt=0.01\ s^{-1}$; $P_{relaxation}$=1 kPa; no wetting …….……. 66

Figure 4.10 Model fits on experimental results for 8W; dε/dt=0.01 s^{-1}; $P_{relaxation}$=1 kPa..67

Figure 4.11 Model fits on experimental results for 8W; dε/dt=0.02 s^{-1}; $P_{relaxation}$=1 kPa..68

Figure 4.12 Model fits on experimental results for 8W; dε/dt=0.005 s^{-1}; $P_{relaxation}$=1 kPa 69

Figure 4.13 Model fits on experimental results for 8W; dε/dt=0.01 s^{-1}; $P_{relaxation}$=5 kPa..70

Figure 4.14 Model fits on experimental results for 8W; dε/dt=0.01 s^{-1}; $P_{relaxation}$=10 kPa 71

Figure 4.15 Model fits on experimental results for 8W; dε/dt=0.01 s^{-1}; $P_{relaxation}$=40 kPa 72

NOMENCLATURE

ε	Strain of the fabric preform
ε_{1S}	Strain in the linear spring element of the model
ε_{1D}	Strain in the damping element of the model
σ_0	Stress in the non-linear spring element of the model [kPa]
σ_{1S}	Stress in the linear spring element of the model [kPa]
σ_{1D}	Stress in the damping element of the model [kPa]
ρ	Superficial density of e-glass fabrics [g/m^2]
$d\varepsilon/dt$	The rate of change of strain [s^{-1}]
dP_c/dt	The rate of change in compaction pressure [kPa/s]
e(t)	The error evaluated during the PID constants iteration
h	The thickness of the specimen [mm]
h_0	The initial thickness of the specimen [mm]
K_d	The derivative constant of the PID controller
K_i	The integration constant of the PID controller
K_p	The proportional constant of the PID controller
m	Weight of e-glass fabrics [g]
P_{atm}	Atmospheric pressure [kPa]
P_c	Compaction pressure [kPa]
P_r	Resin pressure [kPa]
$P_{relaxation}$	Relaxation ressure [kPa]
P_{vac}	Vacuum pressure [kPa]
u(t)	The output of the PID controller
V_f	Fiber volume fraction

Chapter 1

INTRODUCTION

1.1 Vacuum Infusion (VI) Process

Vacuum Infusion (VI) (a.k.a. Vacuum Assisted Resin Transfer Molding (VARTM)) process is a technique that uses vacuum pressure to drive resin into a mold to saturate the previously compacted reinforcement material. A vacuum bag is used as the upper part. When the vacuum is applied to the mold, pressure differential between outer atmospheric and inner vacuum pressure applies compaction pressure on the vacuum bag and the reinforcement material underneath it. The resin is forced to flow through the compacted and porous fiber preform in the mold cavity because of the vacuum. When compared to the other composite manufacturing processes, VI holds a good position with its low cost and ability to manufacture large parts. VI is preferred especially in automotive and marine industries for manufacturing of parts not requiring high surface finish and small dimensional tolerances.

1.2. Variation of Part Thickness (both Spatially and with Time) during VI Process

The variation of part thickness is one of the major issues in VI process. The studies related to this subject are focused on relating the thickness (h) and compaction pressure

(P_c). In the pre-injection stage of VI, P_c is defined as the difference between the atmospheric pressure and the vacuum pressure

$$P_c = P_{atm} - P_{vac} \qquad (1)$$

since the pressure inside the mold is set to P_{vac} by vacuuming it long enough. After the injection is started, Equation (2) replaces Equation (1) at the filled parts.

$$P_c = P_{atm} - P_r \qquad (2)$$

The study of Yenilmez et al. [1] states that the variation of part thickness depends on 3 issues of VI process : (i) as the resin flows through the reinforcement, the resin pressure varies spatially along the flow direction, therefore the compaction pressure varies as well as seen in Equations (1) and (2); (ii) gelation and initial duration of vacuuming also affect the thickness variation; and (iii) the resin may shrink as it cures which is an important factor for thickness variation.

In VI, the resin is stored in an injection tank at atmospheric pressure, and the exit (which is also known as vent) is kept at vacuum pressure. Due to the pressure differential between the inlet gate(s) and the exit(s), the resin is enforced to flow from the inlet to the exit through a porous fiber preform. During mold filling, the resin pressure is maximum at the inlet, and minimum at the flow front (the pressure at the flow front is practically equal to the ventilation pressure). As given in Equation (2), the maximum and the minimum of compaction pressures occur at the opposite points, i.e., it is minimum at the inlet, and

maximum at the exit. P_c is indeed the stress acting on the fiber preform to compact it between the lower mold part and the upper vacuum bag. Due to the spatially varying P_c, the part thickness varies very significantly as also observed and studied in Yenilmez and Sozer's papers [1, 2].

1.3. Compaction Characterization Experiments in the Literature

In some applications such as manufacturing of composite wind turbine blades, the dimensional tolerance in part thickness may not need to be small; thus a significant variation in the part thickness may be acceptable. However, in applications such as automotive parts, not only the surface roughness but also the dimensional tolerance must be small enough. An engineer will benefit from the compaction modeling of VI process, especially by coupling it with the resin flow model. In that compaction modeling approach, one will need to relate the part thickness (and thus the fiber volume fraction) or the true strain to the compaction pressure. In the literature, there have been two different approaches used: (i) the thickness (or its strain) is the independent variable, and the stress is the dependent variable [3]; and (ii) the opposite (the stress is independent, and the strain is dependent) [2] claiming that this approach better mimics the nature of fiber compaction in VI than the former approach considering the stages of the process. This study contributes to the modeling of the VI process by investigating two material characterization procedures for the strain rate controlled experiments. The further study related to the comparison of

those two approaches given above is done in Yenilmez's Phd thesis [4]. The solution of a compaction model may allow an engineer to predict the final thickness and its tolerance, and thus decide on the appropriate control actions to be taken to reduce the variation in the thickness. In Yenilmez's thesis [4], the details of the viscoelastic compaction model is given. In Akyol's thesis [5], the control actions for 1D and 2D resin flows coupled with compaction model are illustrated for sample case studies. This thesis will be useful for the following items: (i) construction of compaction databases for two different fiber preforms and their statistical analysis; (ii) comparisons of the two different control approaches (pressure-rate and strain-rate controlled), and (iii) major guidelines to the model users so that appropriate model parameters and selection of the control approach during the material characterization.

In the literature, there are experimental studies and models to characterize the relationship between the compaction pressure and the thickness or fiber volume fraction (V_f). Yenilmez and Sozer [2] performed compaction characterization experiments for three types of e-glass fabrics (woven, biaxial and random). A distribution medium made of polypropylene material core was also tested alone and as an embedded layer in a fabric sandwich by Yenilmez and Sozer. They used different fabric layup configurations such as 8F, 8F, 8F, 4F1C4F, 2F1C4F1C2F etc. where F stands for the fabric (random, woven or biaxial) and C stands for the core material while the numbers represent the layers. Compaction characterization experiments in the literature are generally focused on woven

types of e-glass fabric preforms. Saunders et al. [6] used 4 types of e-glass woven fabrics (plain, twill, 5 harness satin and non-crimped stitch-bonded e-glass fabric) in their compaction characterization experiments. Chen et al. [7] also used e-glass woven fabrics. There are other studies that are focused on different types of fabrics. For example, stitched random fabric type was used by Yenilmez et al. in their study [1]. Besides that, Bickerton et al. [8] tested continuous filament mat (CFM) as the reinforcement material in their study.

The procedure of the compaction characterization experiments should mimic the actual VI process according to Yenilmez and Sozer [2]. They suggest that dry (or wet) characterization experiments alone do not solely represent VI. Therefore, they started their experiments with a dry preform and wetted it after the settling stage under the major compaction pressure of 100 kPa. Govignon et al. [9] characterized the fiber compaction in the actual VI process as explained below during different stages. They first applied dry loading and dry unloading to a preform. After one cycle, the dry loading was applied again. The wetting occurred after the settling of the second loading. Finally, they performed the wet unloading. Their first cycle (dry loading and dry unloading) mimics the fabric compaction during the search of leakage along sealant which is followed by an actual VI process. Similar to Govignon et al., Yuexin et al. [10] also performed their wet experiments after one cycle of dry experiments. The only difference is that they saturated the preform at the beginning of the second cycle. Therefore, they seperately performed dry and wet experiments which do not fully represent the actual VI according to Yenilmez and Sozer's

claim [2]. There are several other studies in the literature consisting of seperate dry and wet compaction characterization experiments conducted in the same single study [3, 6, 11, 12]. Somashekar et al., Bickerton et al. and Luo et al. performed dry experiments only [8, 13, 14].

There are several types of test fluid in wet or dry/wet experiments in the literature. The most common test fluid is an actual thermoset resin which was used in some studies such as [1, 2, 6, 11]. Yuexin et al. [10] used salad oil as a test fluid in their study. Another test fluid is glucose syrup used in studies such as Kelly et al.'s study [3]. Glucose syrup will be used in this study because of its convenience for cleaning after demolding the specimen; it will be further described in the following section.

In the literature, most commonly applied control approach in a compaction characterization is strain rate controlled experiments as it was done in the universal tensile tests in which strain rate is specified and corresponding stress is measured. But as explained in Yenilmez and Sozer [2], this approach does not mimic the actual VI process's nature. Because, in VI the resin pressure changes as it propagates, and consequently thickness varies. In other words, thickness is dependent on pressure, and not vice versa. According to this claim, Yenilmez and Sozer performed their characterization experiments with pressure rate controlled experiments. There are several other studies in the literature that performed pressure rate controlled experiments [1, 7, 9, 10, 15]. As indicated before, Govignon et al. [9] also tried to mimic the VI process in their compaction characterization experiments,

therefore they performed pressure rate controlled experiments with a maximum of 100 kPa compaction pressure using a tensile test machine as their experimental setup. There are some other studies with strain rate controlled experiments for compaction characterization [3, 6, 8, 11-14].

1.4. Objective

In this study, we will examine the results of strain rate controlled characterization experiments. Model parameters such as stiffness and damper coefficients of a standard linear solid model will be evaluated in strain rate controlled characterization. Those parameters and their responses will be compared with the results of actual VI process in [4].

Chapter 2

EXPERIMENTAL SETUP AND PROCEDURE

2.1. Experimental Setup

The compaction characterization setup, which is simply a VI setup with the addition of a resin distribution layer underneath the preform, is shown in Figure 2.1. The lower side of the mold is an assembly of a galvanized steel plate and acrylic as seen in Figure 2.1. The acrylic part, which consists of the injection and ventilation ports, is seen in Figure 2.2.

The slots on the acrylic part (each having a width of 1.5 mm) and the injection chamber help to reduce the injection time of the resin into the fabric specimen. Injection occurs in 5 stages as seen in Figure 2.3: (i) the test fluid comes inside from the injection point, (ii) fills the injection chamber (because there is no flow resistance in the injection chamber compared with the fabric preform), (iii) then it goes to the slots of the acrylic part (which are partially under the fabric preform), (iv) saturates the fabric with radial injection and (v) completely fills the mold cavity. The width of the injection chamber is an important issue for the injection time. It should be wide enough to allow the fluid flow, but narrow enough to prevent the vacuum bag to stick to the injection chamber under vacuum (which prevents the fluid flow). After some trial-and-error experiments with prototypes, the width

of the injection chamber was selected as 3 mm satisfying the complete wetting of the specimen in shorter than 15 seconds, and also preventing the collapse of the bag on the chamber.

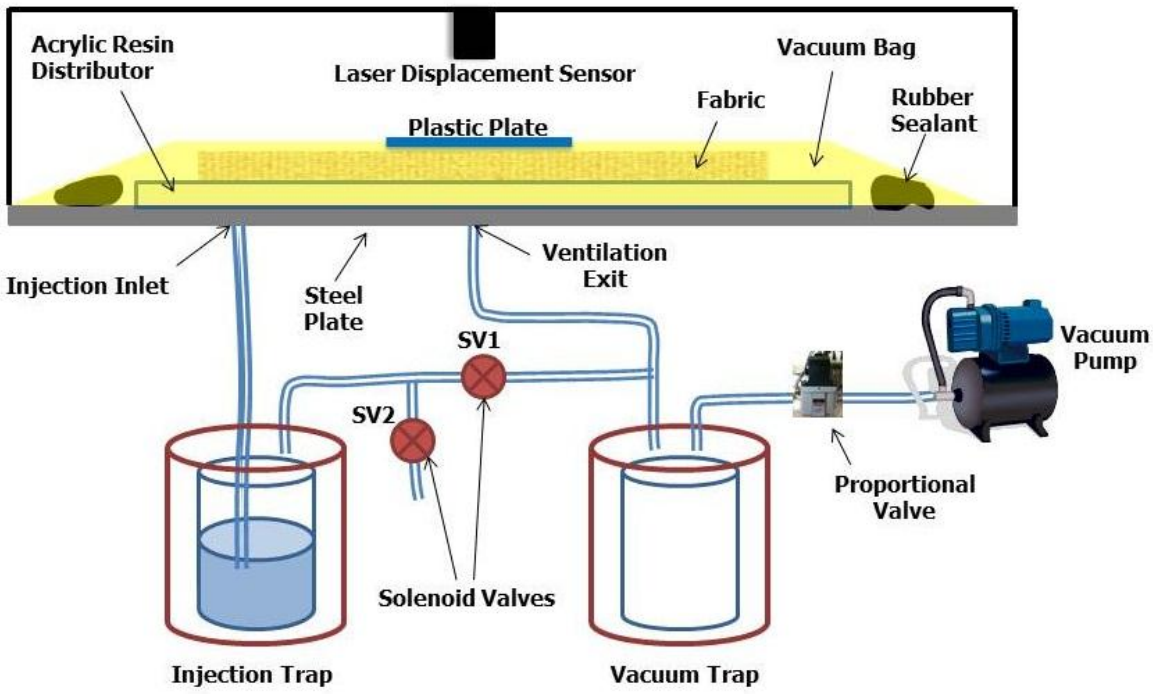

Figure 2.1. Schematic of the experimental setup

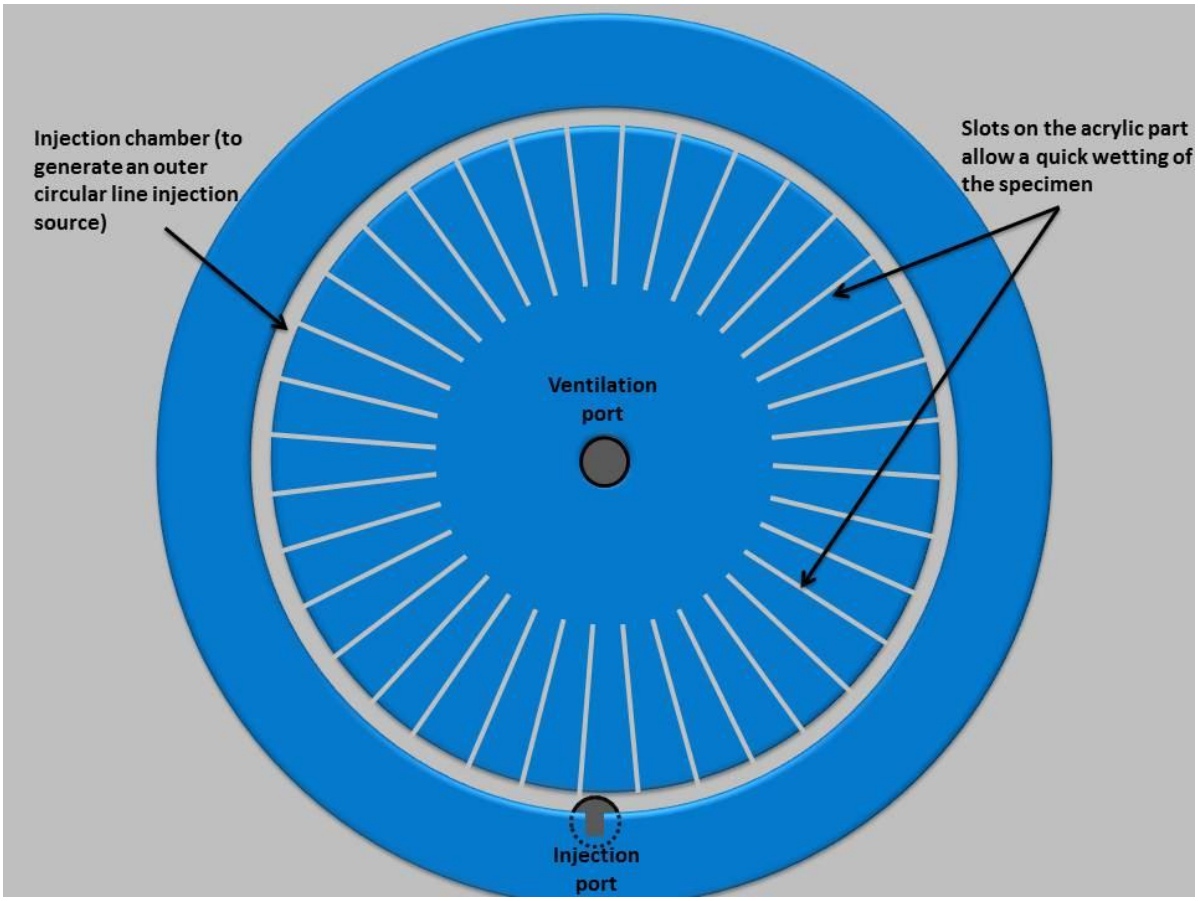

Figure 2.2. Acrylic resin distributor assembled on the steel plate

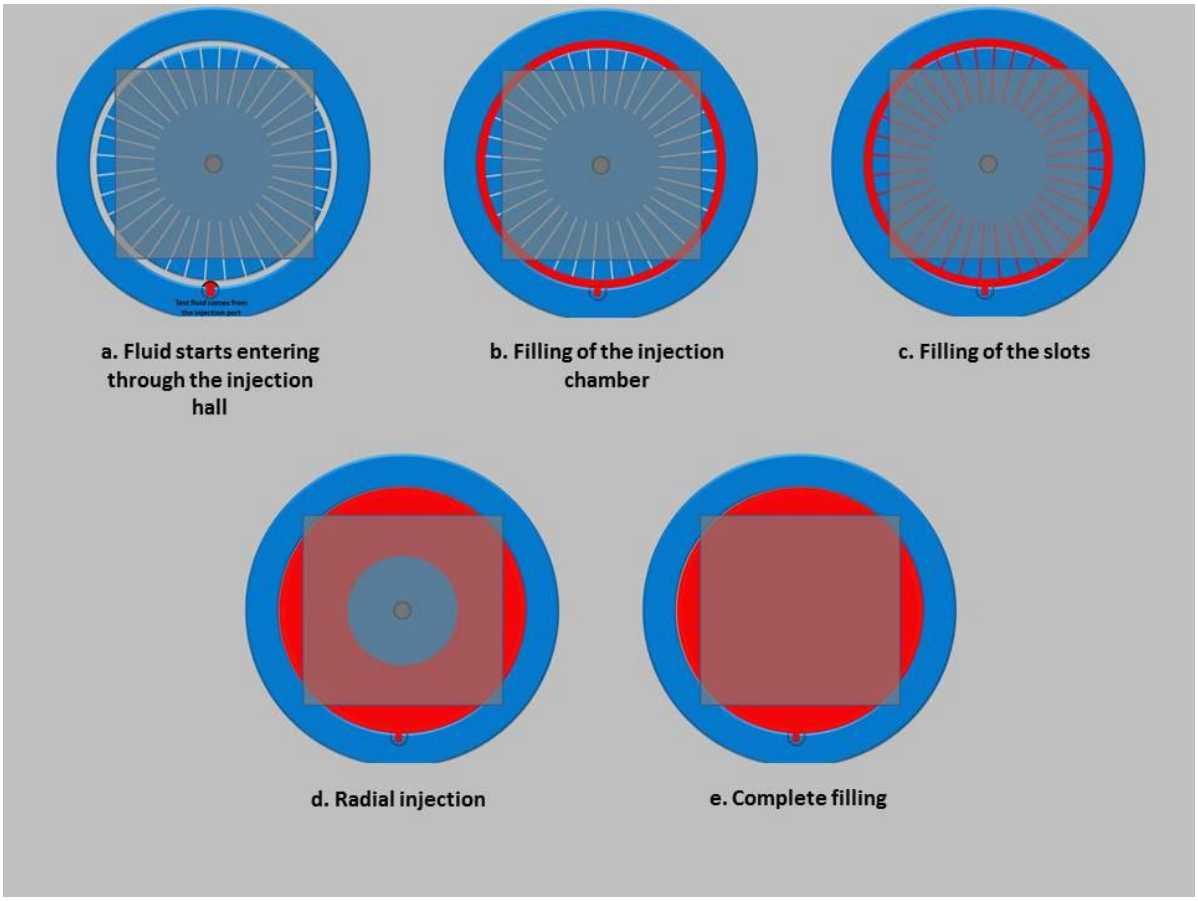

Figure 2.3. Illustration of wetting of the specimen

As seen in Figure 2.3, the specimen is unsaturated at the corners, but it does not affect the thickness or compaction pressure. Because, compaction pressure does not change with the area of the specimen (unlike tensile test machine which applies compaction force to obtain compaction pressure) and the thickness of the specimen is monitored at the center of it (from the center of the plastic plate seen in Figures 2.4(a-c).

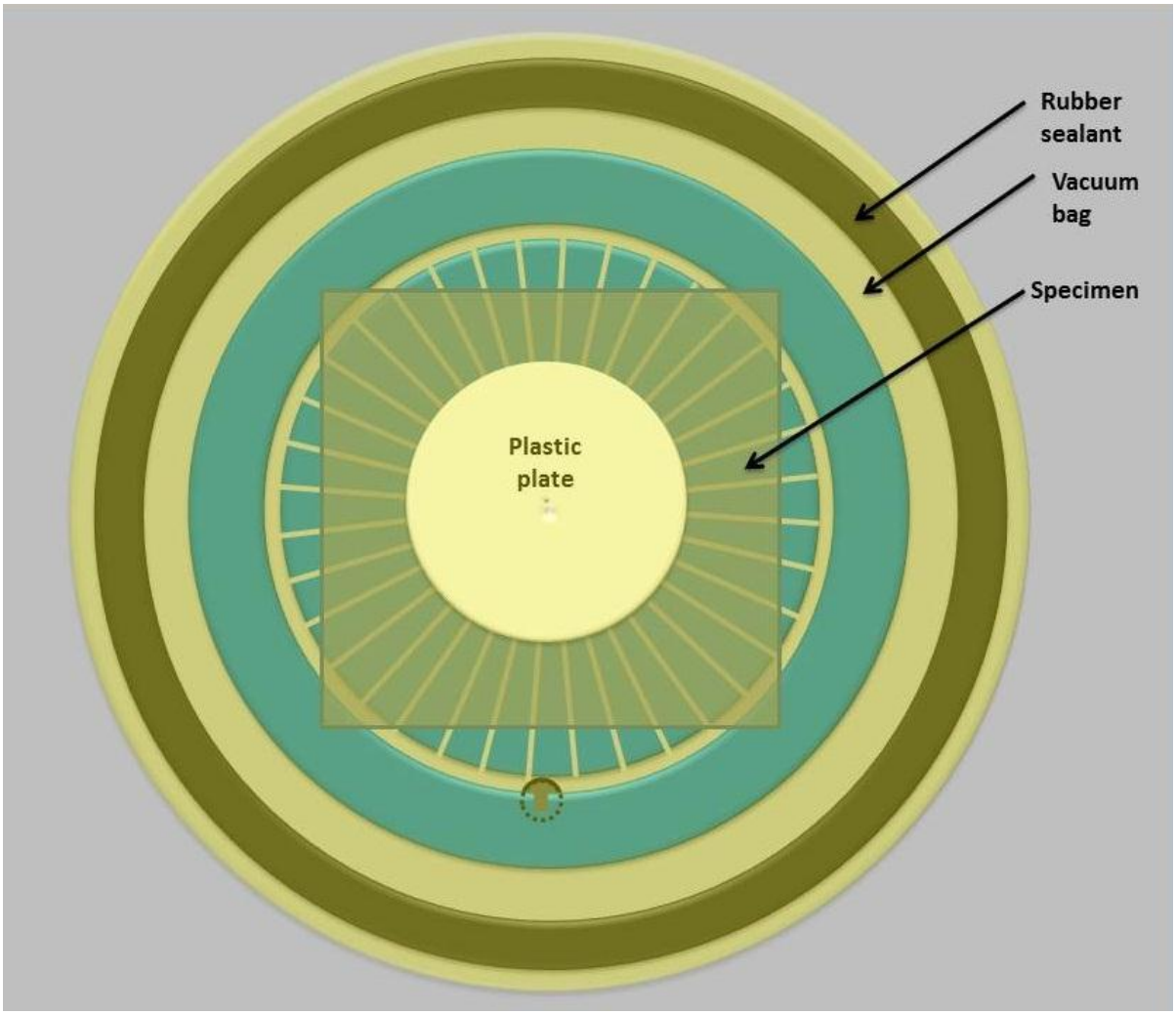

Figure 2.4.(a). Specimen placed on the experimental setup (top view)

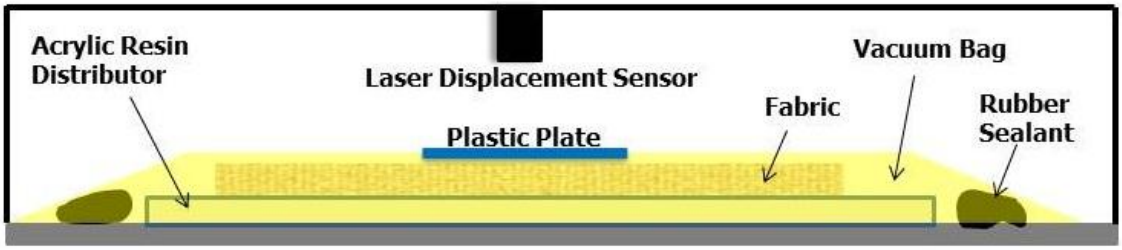

Figure 2.4.(b). Specimen placed on the experimental setup (side view)

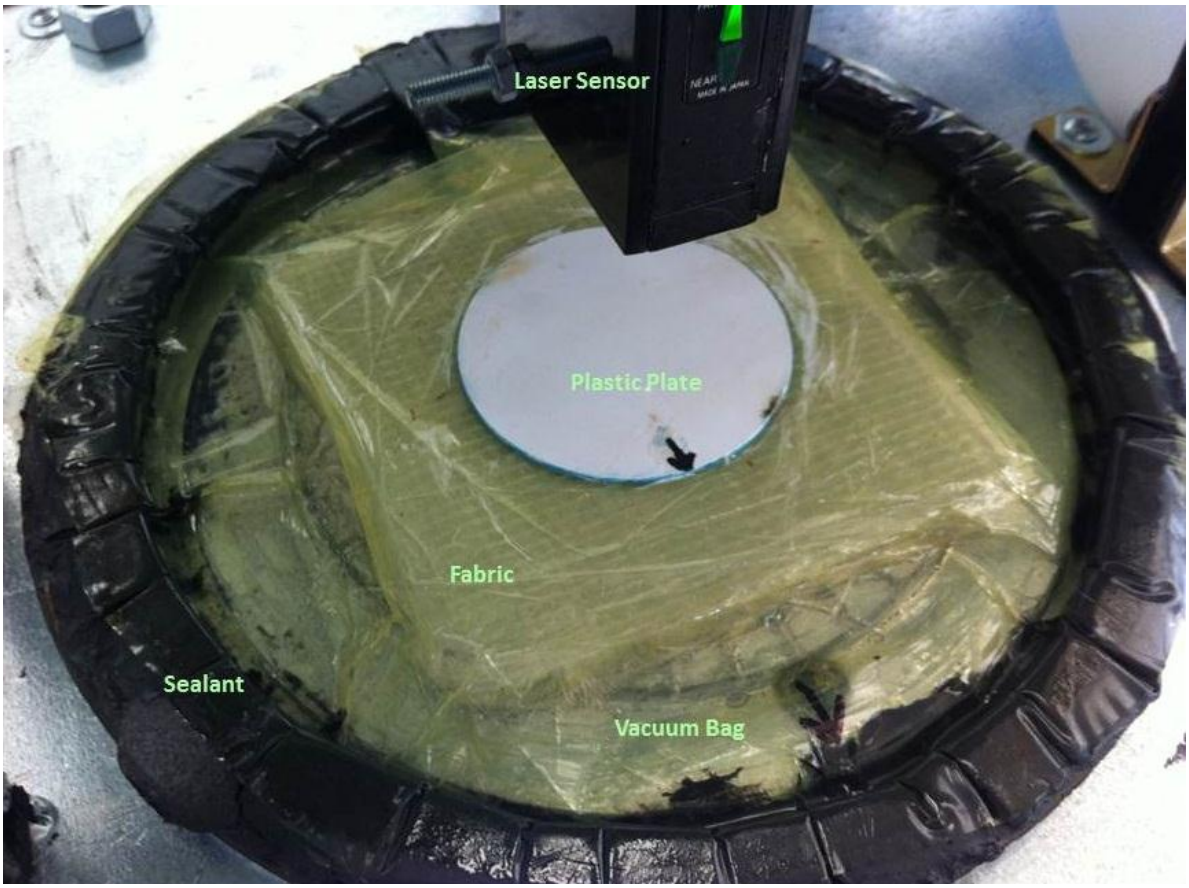

Figure 2.4.(c). Specimen placed on the experimental setup (photograph)

The upper side of the mold is a vacuum bag as shown in Figures 2.4(a-c). An Omron Z4M-W40 laser displacement sensor (having a resolution of 1.5 μm) is placed above the mold to monitor the thickness of the specimen during the experiment. The plastic plate seen in Figures 2.4(a-c) (which is stuck to the vacuum bag) helps to read the thickness more properly because, (i) it provides uniformity in thickness of the specimen, and (ii) the laser displacement sensor can read white color surfaces with less noise compared to shiny surface of a vacuum bag. A proportional valve is connected to a vacuum pump (Alcatel Pascal 2010 SD) to control the vacuum pressure using a PID (Proportional, Integral and Derivative) control system which has a block diagram as seen in Figure 2.5. The actual pressure is measured by the pressure sensor connected to the proportional valve. The measured pressure is used as the feedback value in the PID control system. The difference between the desired pressure and the actual pressure is calculated and called the error. The PID constants, which are determined via manual tuning (with a trial-and-error approach which is going to be explained in the following sub-section), try to minimize this error by sending information based on the error itself to the proportional valve on how much it should be open. The PID equation used in the block diagrams is given below [16]

$$u(t) = K_p e(t) + K_d \frac{de(t)}{dt} + K_i \int_0^t e(t)dt \qquad (3)$$

where u(t) is the output, e(t) is the error and K_p, K_d, K_i are the PID constants to be determined by manual tuning.

All the components of the setup are connected to CPU via data acquisition (DAQ). Thus, the setup performs the experiments with full automation including the injection stage by controlling the solenoid valves (SV1 & SV2) shown in Figure 2.1. During the stages that injection is not continued, SV1 is open and SV2 is closed. Thus, injection and vacuum traps have the same vacuum pressure. Under this condition, the injection does not occur, because there is no pressure difference between the inlet and the ventilation. When the injection is continued, SV1 is closed and SV2 is open which results in the atmospheric pressure inside the injection trap while the vacuum trap has vacuum pressure. This difference allows the fluid to flow from the injection trap to the mold.

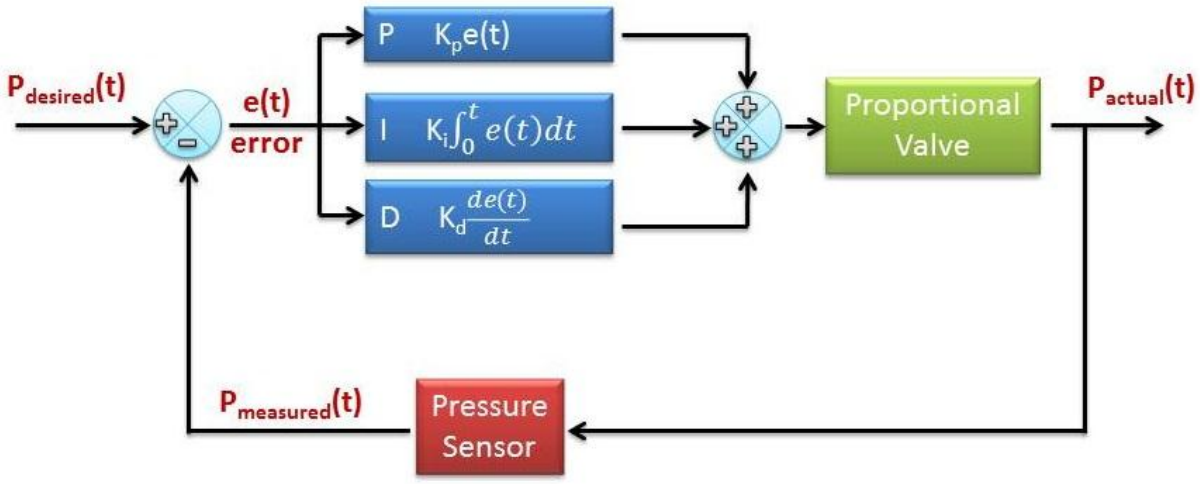

Figure 2.5. Block diagram of PID control system for pressure rate controlled experiments

The experimental setup is able to perform two types of controlled experiments: (i) pressure rate controlled (where compaction pressure is controlled and corresponding strain or thickness is measured) and (ii) strain rate controlled (where strain or thickness is controlled and the corresponding pressure is measured). The PID control system shown in Figure 2.5 allows performing pressure rate controlled experiments. For strain rate controlled experiments, the PID control system runs as shown in Figure 2.6. The controlled component is the same as the previous one (which is the proportional valve), but instead of the pressure sensor, the laser displacement sensor is used as the feedback mechanism. The thickness value measured by the sensor is converted to true strain and the difference between the desired and the actual strain is calculated and called as the error.

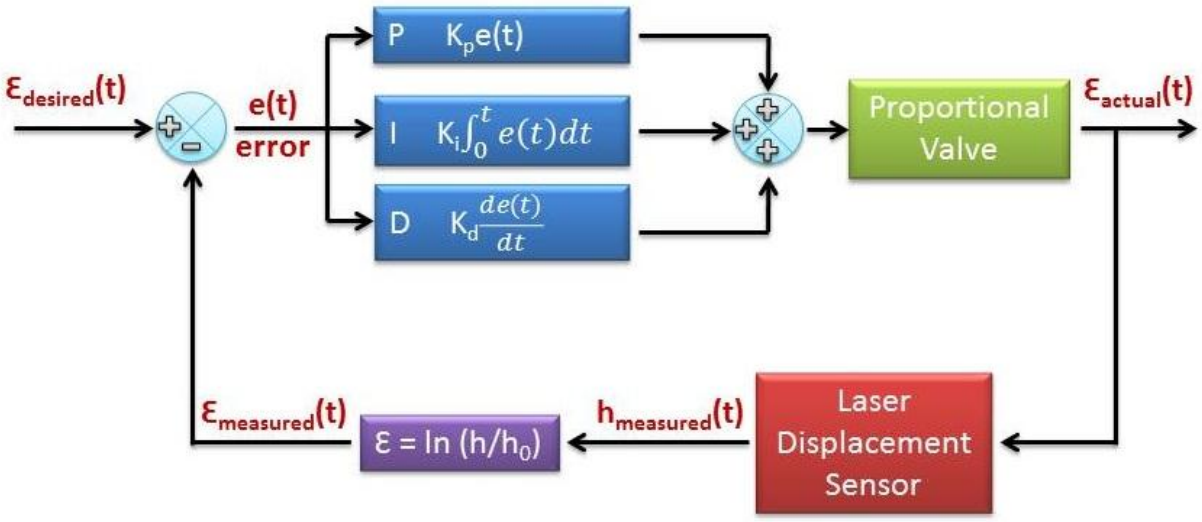

Figure 2.6. Block diagram of PID control system for strain rate controlled experiments

The manual tuning is done by increasing or decreasing the PID constants by observing their effects on the system response as seen in Table 2.1.

Table 2.1. Effects of increasing the PID constants on system response, adapted from [17]

Effects of increasing PID constants on system response	Rise Time	Overshoot	Settling Time	Steady State Error	Stability
Increasing K_p	**Decrease**	**Increase**	**Small Increase**	**Decrease**	**Decrease**
Increasing K_d	**Small Decrease**	**Decrease**	**Decrease**	**Minor Change**	**Increase**
Increasing K_i	**Small Decrease**	**Increase**	**Increase**	**Large Decrease**	**Decrease**

2.1.1. PID Tuning of Pressure Rate Controlled Experiments

The proportional valve seen in Figure 2.1 is connected to both vacuum and atmospheric pressures. In order to adjust the desired compaction pressure, it opens the vacuum or atmospheric gates according to the information send from the feedback PID control mechanism. Firstly, a set of PID constants are determined. According to the system behavior, they are changed based on their effects on the control system as seen in Table 2.1 [17].

The initial PID constants and the corresponding system behavior are seen in Figure 2.7(a); and it is called Case A. The system did not respond fast enough in this case.

Therefore, proportional (K_p) and integration (K_i) constants are increased in Case B; and the system behavior is observe in Figure 2.7(b). The figure shows that the constants need to be increased further according to Table 2.1. In Case C, the PID constants are increased even further, and the system behavior is observed as seen in Figure 2.7(c), which responds fast enough; but the system has stability problems (i.e., the system behavior oscillates around the desired set path). To reduce the oscillations, K_p is reduced; and the other two constants are tuned. After several fine-adjustments, they are determined as in Case D. The system behavior and PID constants are seen in Figure 2.7(d).

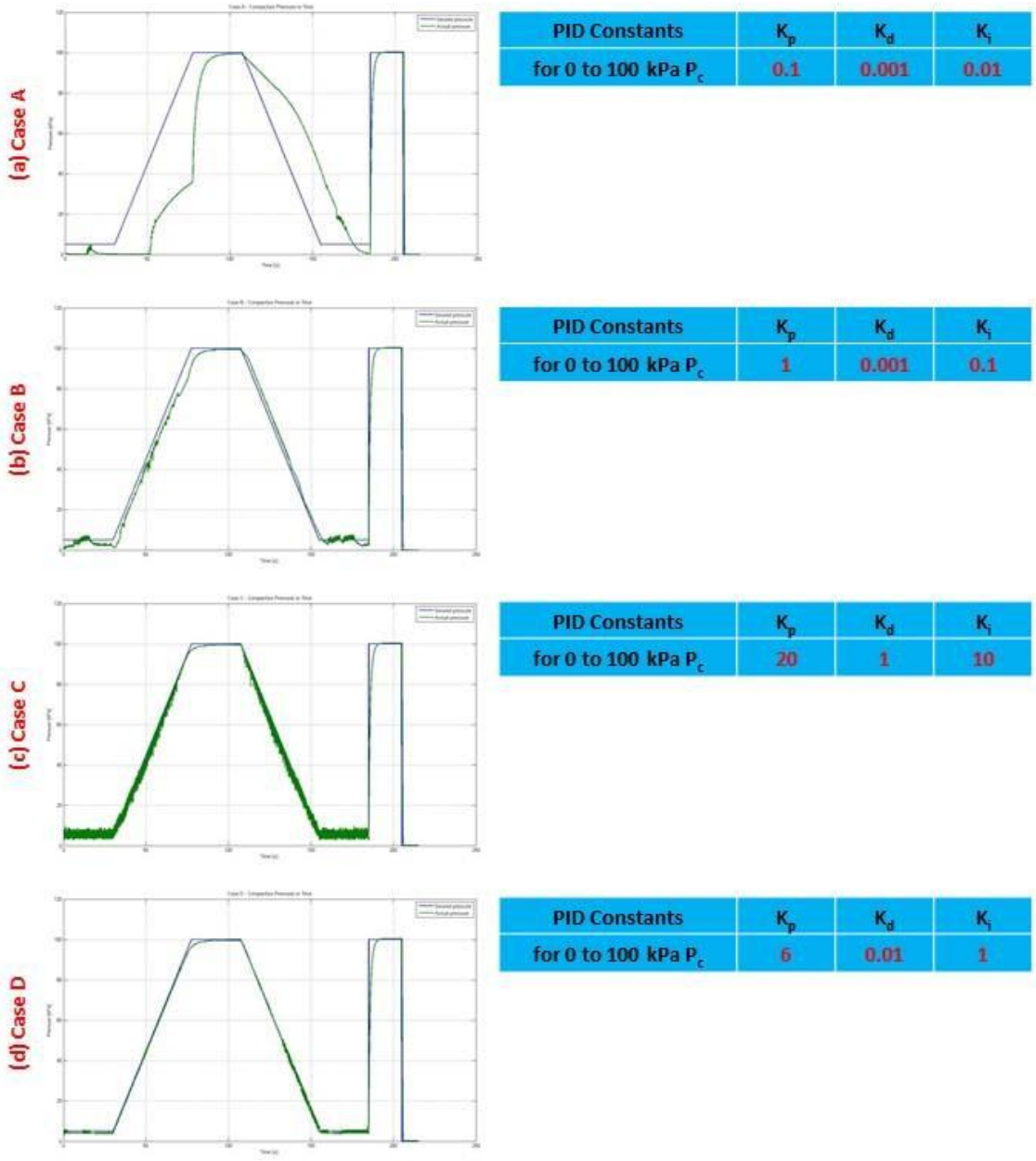

Figure 2.7. PID manual tuning for pressure rate controlled experiments (system behavior for different PID constants). The horizontal axes are time, and the vertical axes are compaction pressure.

2.1.2. PID Tuning of Strain Rate Controlled Experiments

The tuning of PID constants of strain rate controlled experiments is illustrated using several case studies; and five of them are seen in Figure 2.8. In Cases A, B and C, the PID constants are increased as seen in Figures 8(a-c). When comparing the graphs of those three figures, one can conclude that the system has short rise time and low steady-state error as the constants are tuned from Case A to C. However, the oscillations are increased in Case C as seen in Figure 2.8(c). To increase the stability in Case D, by following Table 2.1, K_p and K_i are decreased. Although the other constant, K_d is also suggested to be increased, it is experimentally observed that, the stability was achieved by decreasing it. The graph shown in Figure 2.8(d) shows an acceptable system behavior (except for the stability problems at low pressure values) with the PID constants seen in the same figure. Further fine-adjustments do not provide any further improvements in the stability of the system. The compaction characterization experiments performed by Yenilmez and Sozer [2] suggest that the behavior of e-glass fabrics under compaction is non-linear. Therefore, the PID constants that perform well at low pressures cannot track the desired strain path at high compaction pressures; or the constants that can track the desired strain path at high compaction pressures have stability problems at low pressures. Controllers that can respond to non-linear and higher order systems can give better controlling results when compared to PID controllers [18]. However, to design such controllers, the transfer function of the system is needed, and the transfer function of the compaction behavior of fabrics cannot be

generated before the experiments. Therefore, to determine the non-linear relationship, different stages of characterization experiment are designed as shown in Figure 2.8(e). The corresponding system behavior graph is also seen in the same figure. Note that in each stage, different sets of proportional constants are used to have stability in all stages, as well as short rise time in loading and unloading stages.

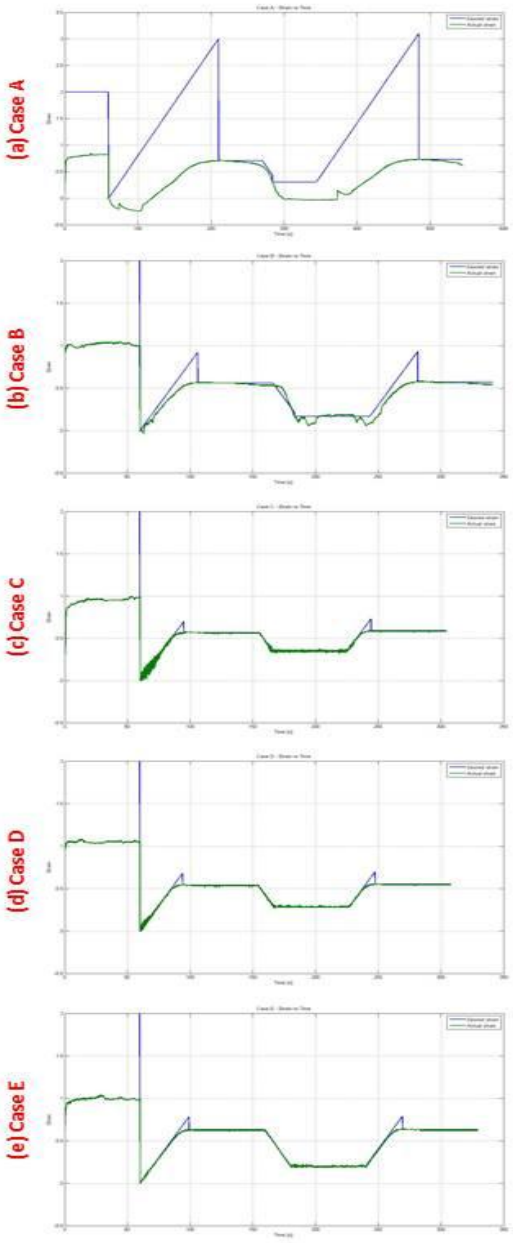

PID Constants	K_p	K_d	K_i
for 0 to 100 kPa P_c	5	2	4

PID Constants	K_p	K_d	K_i
for 0 to 100 kPa P_c	50	2	40

PID Constants	K_p	K_d	K_i
for 0 to 100 kPa P_c	5000	20	4000

PID Constants	K_p	K_d	K_i
for 0 to 100 kPa P_c	500	2	400

PID Constants	K_p	K_d	K_i
for 0 to 5 kPa P_c	120	0.01	240
for 5 to 10 kPa P_c	220	0.01	290
for 5 to 10 kPa P_c	300	0.05	320
for 5 to 10 kPa P_c	585	0.05	520

Figure 2.8. PID manual tuning for strain rate controlled experiments (system behavior for different PID constants). The horizontal axes are time, and the vertical axes are compaction strain.

2.2. Fabrics

There are two types of e-glass fabrics (random and woven) used in this study. The brands and superficial densities of the e-glass fabrics are:

- Random Fabric: 500 g/m^2 , Fibroteks
- Woven Fabric : 500 g/m^2, Fibroteks

The ventilation point seen in Figure 2.2 is at the center of the specimen. The fabric presence on the ventilation point may interrupt the vacuum because of its blockage on the hole. To prevent this problem, fabrics are punched as shown in Figure 2.9.

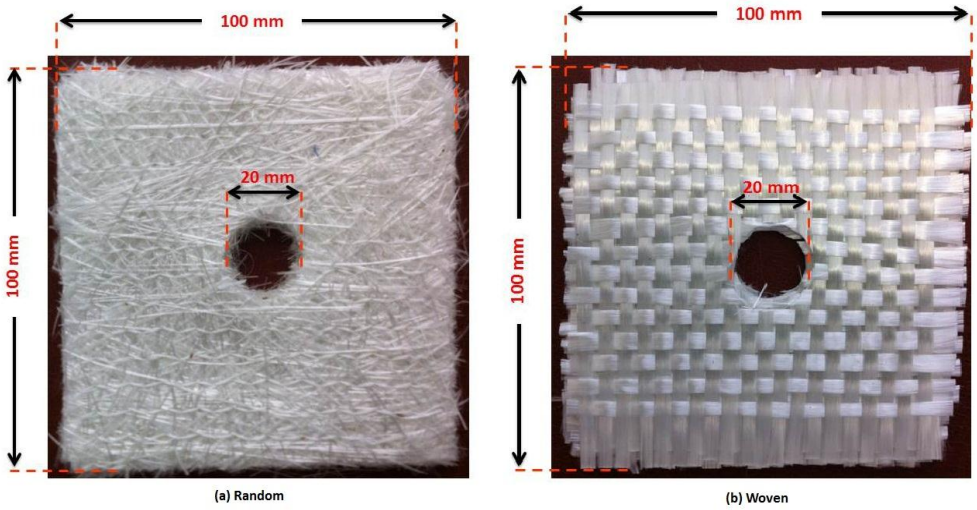

Figure 2.9. E-glass fabrics used in the experiments

There is a variation of real weights and superficial densities of the fabrics used in all the experiments. The max-min, average values and standard deviations of them are given in Table 2.2.

Table 2.2. Weights and superficial densities of the specimens used in the experiments

Fabric Weights and Superficial Densities	m_{max}	m_{min}	m_{mean}	$m_{standard\ deviation}$	ρ_{max}	ρ_{min}	ρ_{mean}	$\rho_{standard\ deviation}$
Random Fabric	44 g	27 g	35.2714 g	3.6392 g	570 g/m^2	348 g/m^2	454.9286 g/m^2	46.7467 g/m^2
Woven Fabric	35 g	30 g	32.6429 g	1.3301 g	452 g/m^2	391 g/m^2	420.3000 g/m^2	16.4831 g/m^2

2.3. Test Fluid

Thermoset polyester resin is used in composite material production in our laboratory, CMML (Composite Materials Manufacturing Laboratory) at Koç University. However, polyester resin is not easy to clean after the experiments since it is sticky before it cures. Glucose syrup diluted with water, which has similar properties with polyester resin is used in this study. Glucose syrup is an incompressible and Newtonian (linear relation between shear stress and viscosity) fluid like polyester resin at low Reynolds number applications such as RTM (Resin Transfer Molding) and VI.

The density of glucose syrup is approximately 1300 g/cm^3 and its viscosity is adjusted to 0.200 Pa.s by diluting it with water and using a viscometer.

2.4. Experimental Procedure

2.4.1. Pre-Experimental Procedure

Certain amount of specimens (enough to perform all of the experiments) are prepared by cutting and stacking eight layers of fabric with the desired dimensions and

punched as shown in Figure 2.9. After the preparation of the specimens, they are left for relaxation for minimum of 2 days (to recover the original thickness after the deformation during cutting/punching).

Before the experiment, the plastic plate and vacuum bag are placed on the mold; and the laser displacement sensor reads the thickness at that instant (this value will be subtracted from the thickness data of the full assembly during the experiment to calculate the thickness of the specimen itself). After this stage, fabric preform is placed on the mold and sealant (the assembly of sealant, vacuum bag and the plastic plate) is placed on the fabric as seen in Figure 2.10. After the injection trap is checked (whether there is enough glucose syrup to perform the experiment or not), the experiment is started.

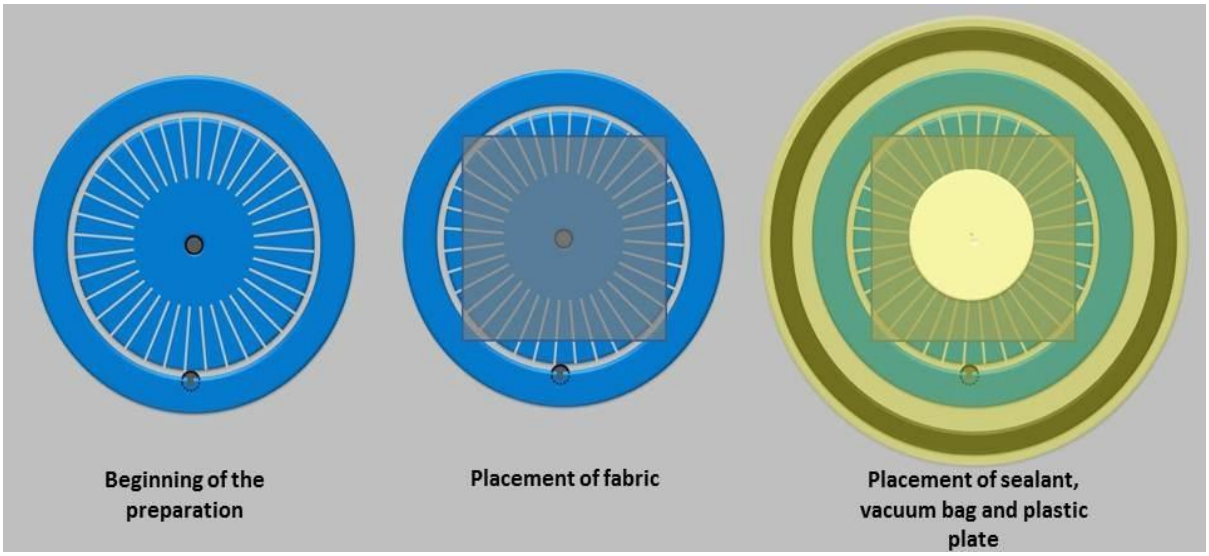

Figure 2.10. Placement of the fabric and vacuum bag during the preparation of the experiment

2.4.2. Pressure Rate Controlled Experiments

The pressure rate controlled experiments are performed in Yenilmez's Phd thesis and the experimental procedure of those experiments is given below.

At the beginning of the pressure rate controlled experiments, the specimen is exposed to a pre-settling stage for 300 seconds under a minor compaction pressure of 1 kPa. One could ideally conduct this part of the characterization at $P_c = 0$ kPa to measure the initial thickness of the undisturbed specimen. However, considering very large variations in the initial specimen thickness due to inconsistencies in the cutting/stacking/storing of the fabric layers, and also mimicking the slight effect of vacuum bagging on the fiber preform in VI, the procedure of the characterization experiments are designed such that the specimen is kept under a minor load of 1 kPa. Besides, there should be ample contact between the bag and the specimen so that the thickness is not mis-measured; and this could not be achieved in $P_c = 0$ (i.e., when no vacuum is applied).

The experimental procedure of the pressure rate controlled experiments is described in Figures 2.11 and 2.12. After the pre-settling stage, a specimen is loaded under constant pressure rates ($dP_c/dt = 2$ kPa/s (will be called nominal experiments), 1 kPa/s and 4 kPa/s) until the loading reaches a major compaction pressure of 100 kPa (this part of the experiment is called loading stage) as shown in Figure 2.12. When P_c reaches 100 kPa, the loading stage ends, and the settling stage starts and lasts for 300 seconds. Except the fully dry experiments (which is performed in only one set for each fabric type at the nominal

pressure rate and relaxation pressure (1 kPa)), fiber wetting occurs during the last 30 seconds of the settling stage. After that stage, specimens are unloaded with constant dP_c/dt until P_c reaches one of the minor compaction pressure values ($P_{relaxation}$ = 1 kPa (nominal), 5 kPa, 10 kPa, 40 kPa) as shown in Figure 2.11. The relaxation stage starts when P_c reaches the minor load and lasts for 300 seconds. Finally, the specimen is compacted with the same pressure rate until it reaches 100 kPa and kept at the major load for 60 seconds to investigate the effect of wet loading and settling stages.

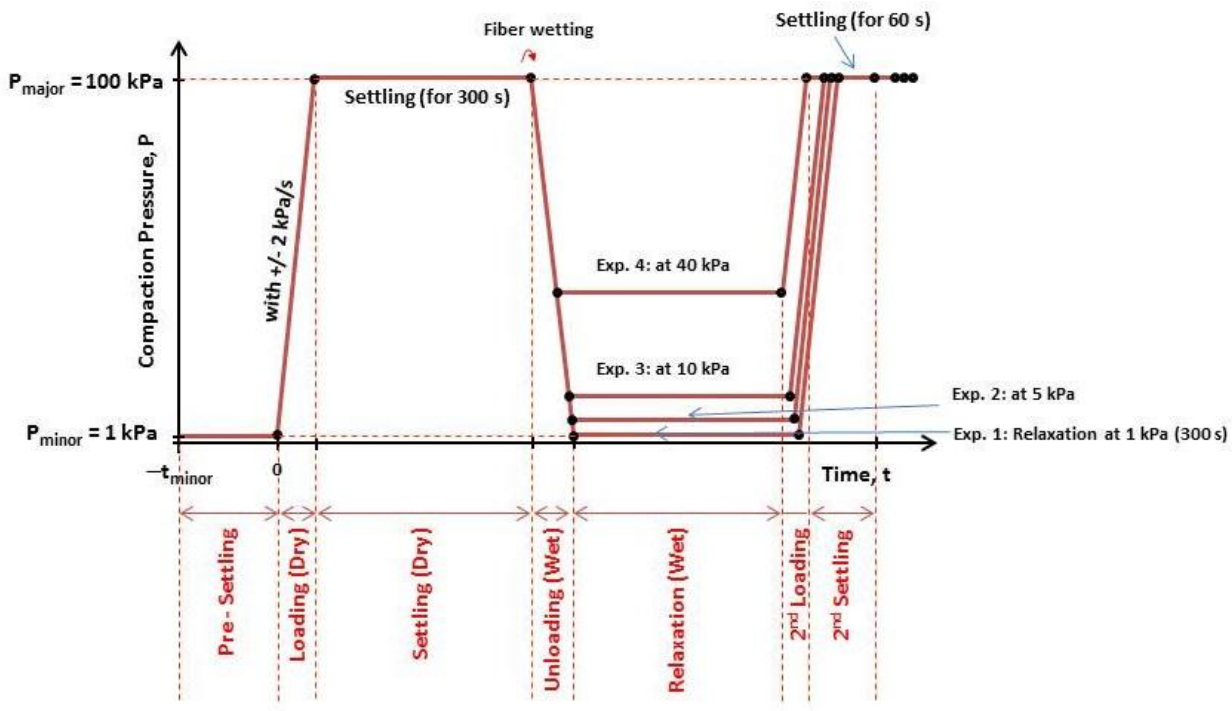

Figure 2.11. Pressure rate controlled characterization experiments by varying $P_{relaxation}$

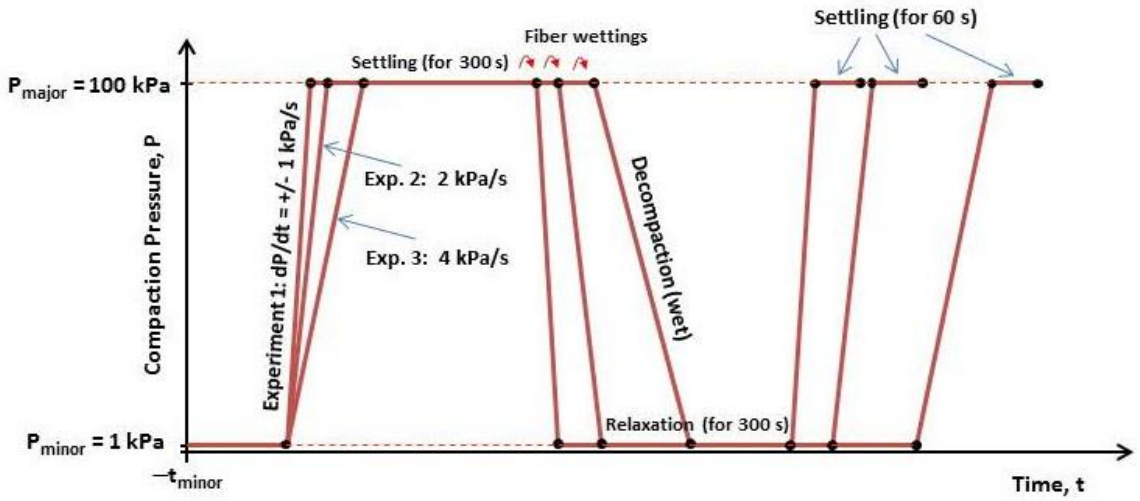

Figure 2.12. Pressure rate controlled characterization experiments by varying dP/dt

As indicated in the first section, e-glass fabrics exhibit viscoelastic behavior under compaction/decompaction characterization experiments [2, 3]. During settling and relaxation stages (for 300 seconds each) the viscoelastic response of the specimens are observed which occur instantaneously and as deformation with time (viscous response). The pressure rate controlled compaction characterization, viscoelastic compaction/decompaction modeling, and curve fit to experimental data are studied in detail in Yenilmez's PhD thesis [4].

2.4.3. Strain Rate Controlled Experiments

Strain rate controlled experiments also start with the pre-settling stage which is exactly the same as the stage studied in pressure rate controlled experiments. All stages of the strain rate controlled experiments can be seen in Figure 2.13.

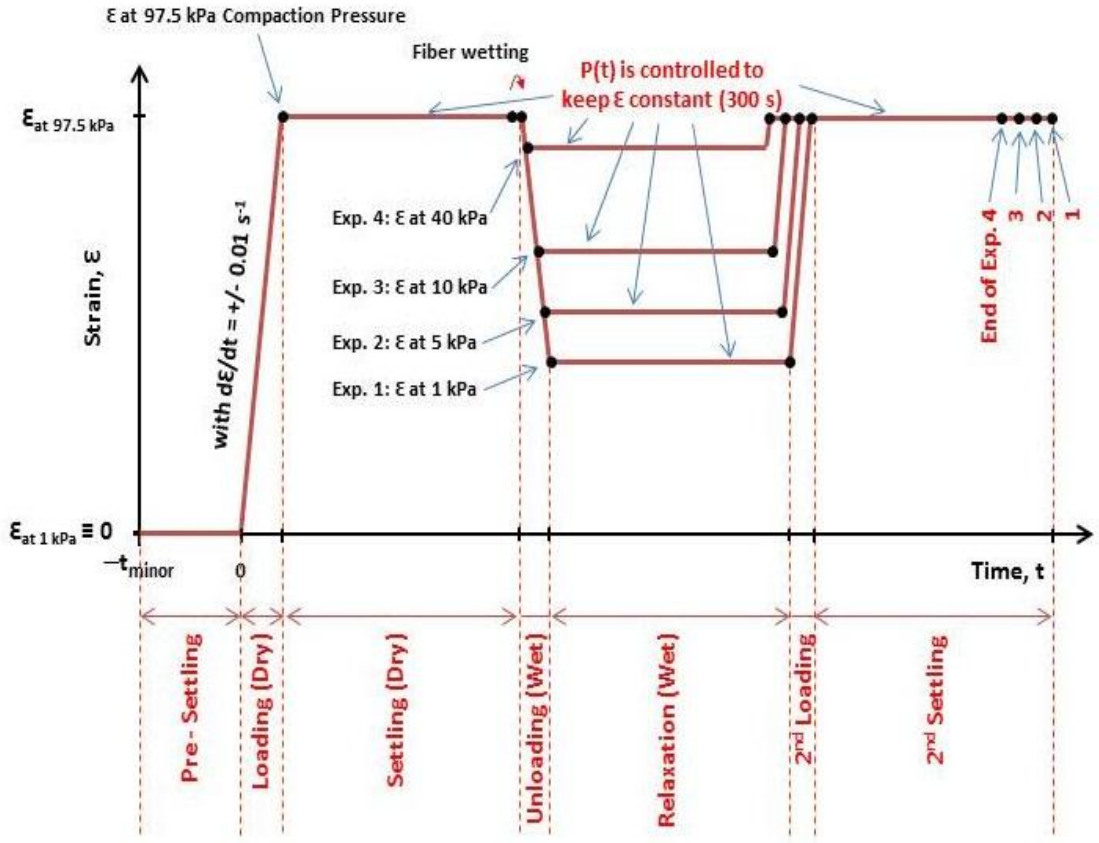

Figure 2.13. Strain rate controlled characterization experiments by varying $P_{relaxation}$

The thickness measured at the end of the pre-settling stage (under minor pressure) is considered as the initial thickness h_0. The true strain during the experiment is calculated using h_0 as $\varepsilon=\ln(h/h_0)$. Therefore, strain is considered as zero at the beginning of the loading stage, and note that absolute strain is considered. During the loading stage, the strain is increased at a constant rate (0.01 s^{-1} (will be called as nominal), 0.005 s^{-1} and 0.02 s^{-1}) until the compaction pressure reaches to 97.5 kPa as shown in Figure 2.14. Due to the capacity of the vacuum pump and proportional valve used, above 97.5 kPa, the pressure rate is very low during strain rate controlled experiments. Consequently, the compaction pressure cannot reach 100 kPa with the selected constant strain rates. Thus the characterization procedure is designed such that the major compaction pressure is set to 97.5 kPa instead of 100 kPa. The strain is monitored, and when P_c reaches 97.5 kPa, the strain is constant at the corresponding value recorded at that instant. To keep the strain constant, the compaction pressure is decreased gradually (which will be called as pressure relaxation) because of the viscoelastic properties of e-glass fabric. During the last 30 seconds of this settling time (which is 300 seconds), the specimen is saturated with the test fluid. After wetting of the specimen, the strain is decreased with the same absolute rate as it was increased until the compaction pressure reaches one of the minor load values chosen (which are the same as in the pressure rate controlled experiments) as it can be seen in Figure 2.13. In the relaxation stage, the strain (which is the first strain when P_c reached the

minor load value) is kept constant for 300 seconds. After that stage, loading and settling is repeated to see the effect of wetting on these stages.

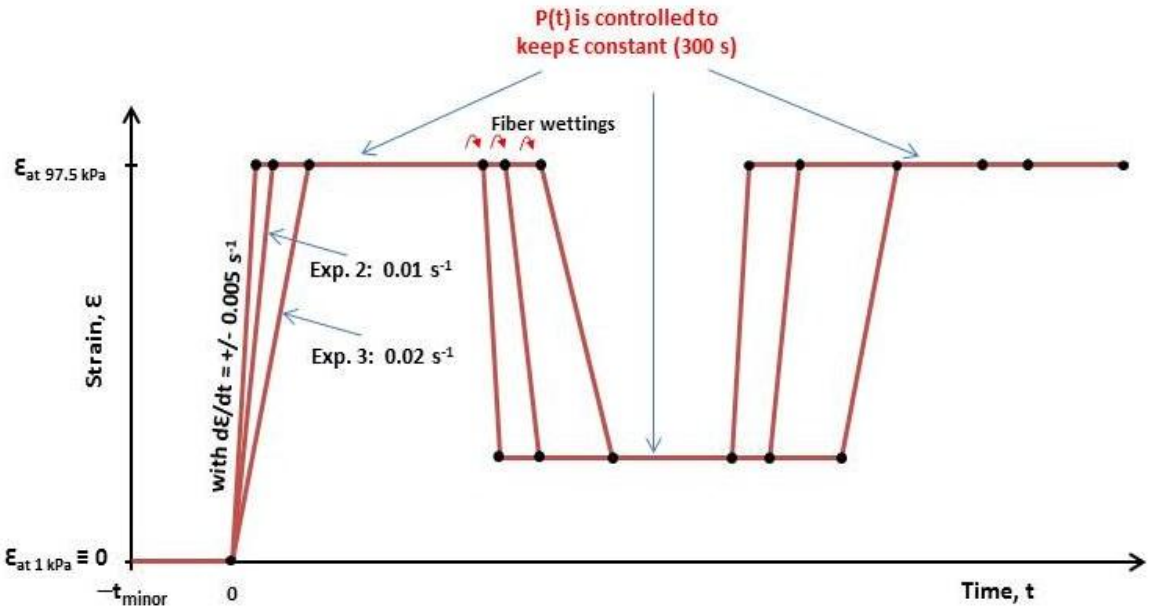

Figure 2.14. Strain rate controlled characterization experiments by varying dƐ/dt

This study aims to provide a database for strain rate controlled compaction characterization to compare the two types of experiments performed in the literature (pressure rate and strain rate controlled). Therefore, the experimental procedures are kept very similar in both types of controlled experiments so that the results of two approaches can be compared under fair conditions.

Chapter 3

EXPERIMENTAL RESULTS

The compaction characterization experiments are conducted for two fabric types (random and woven) as discussed in the previous chapters. The results for random fabric type are seen in Figures 3.1 - 3.7 and the results for woven type are seen in Figures 3.8 - 3.14.

As discussed earlier in this thesis, for each fabric type, characterization is conducted by using different values of $d\varepsilon/dt$ and $P_{relaxation}$. Therefore, the results are organised in that fashion as indicated in Tables 3.1 and 3.2.

Table 3.1. The list of figures showing experimental results for random fabric with different experimental procedures such as varying $d\varepsilon/dt$ and $P_{relaxation}$ values, and wetting condition

Random Fabric	**$d\varepsilon/dt$**	**$P_{relaxation}$**	**Wetting**
Figure 3.1	0.01 s^{-1}	1 kPa	✘
Figure 3.2	0.01 s^{-1}	1 kPa	✓
Figure 3.3	0.02 s^{-1}	1 kPa	✓
Figure 3.4	0.005 s^{-1}	1 kPa	✓
Figure 3.5	0.01 s^{-1}	5 kPa	✓
Figure 3.6	0.01 s^{-1}	10 kPa	✓
Figure 3.7	0.01 s^{-1}	40 kPa	✓

Table 3.2. The list of figures showing experimental results for woven fabric with different experimental procedures such as varying dε/dt and $P_{relaxation}$ values, and wetting condition

Woven Fabric	**dε/dt**	**$P_{relaxation}$**	**Wetting**
Figure 3.8	0.01 s^{-1}	1 kPa	✘
Figure 3.9	0.01 s^{-1}	1 kPa	✓
Figure 3.10	0.02 s^{-1}	1 kPa	✓
Figure 3.11	0.005 s^{-1}	1 kPa	✓
Figure 3.12	0.01 s^{-1}	5 kPa	✓
Figure 3.13	0.01 s^{-1}	10 kPa	✓
Figure 3.14	0.01 s^{-1}	40 kPa	✓

In each set (e.g. in Figure 3.1), ten experiments are conducted to investigate the statistical variation among the specimens.

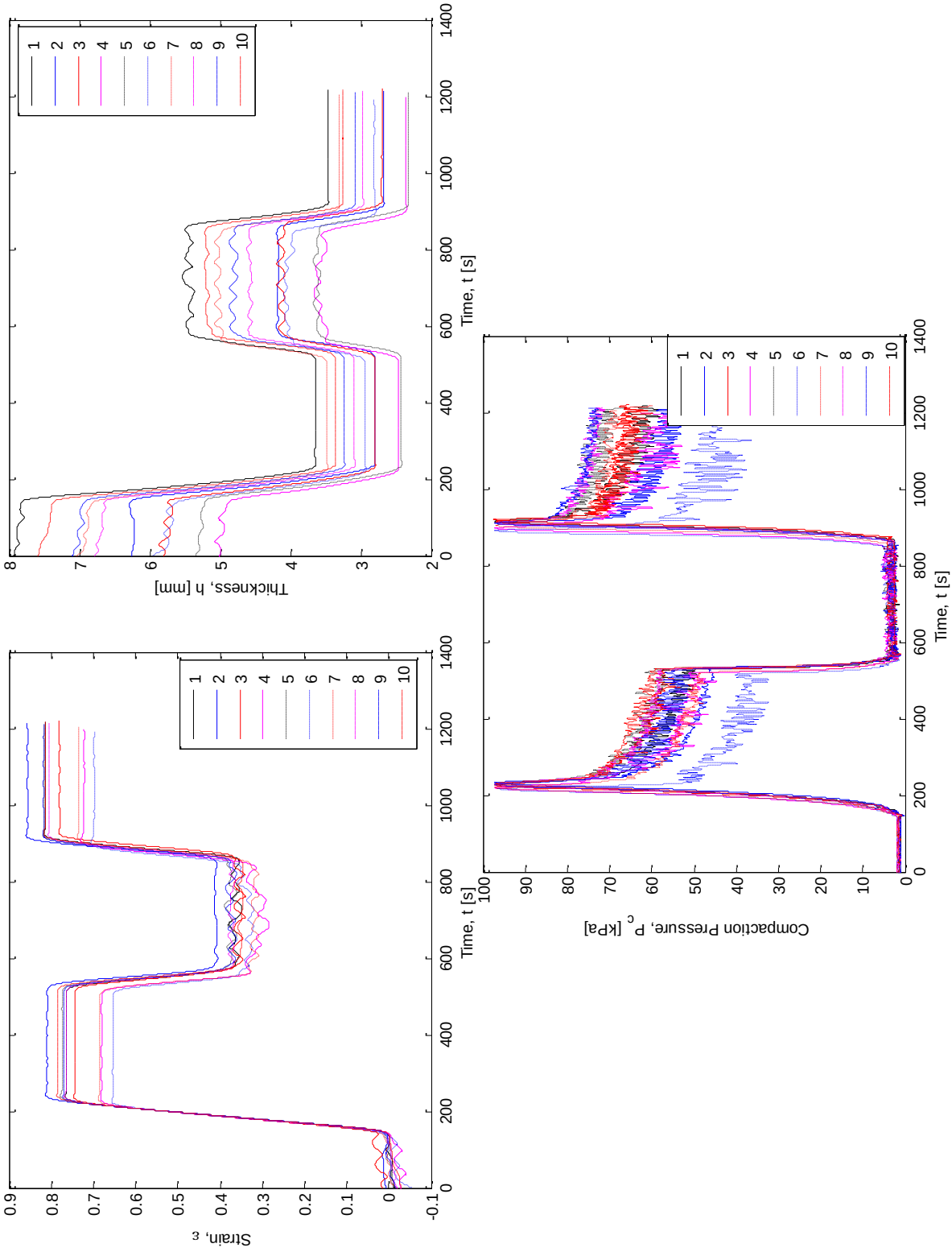

Figure 3.1. Experimental results for 8R; $d\varepsilon/dt = 0.01\ s^{-1}$; $P_{relaxation} = 1$ kPa; no wetting

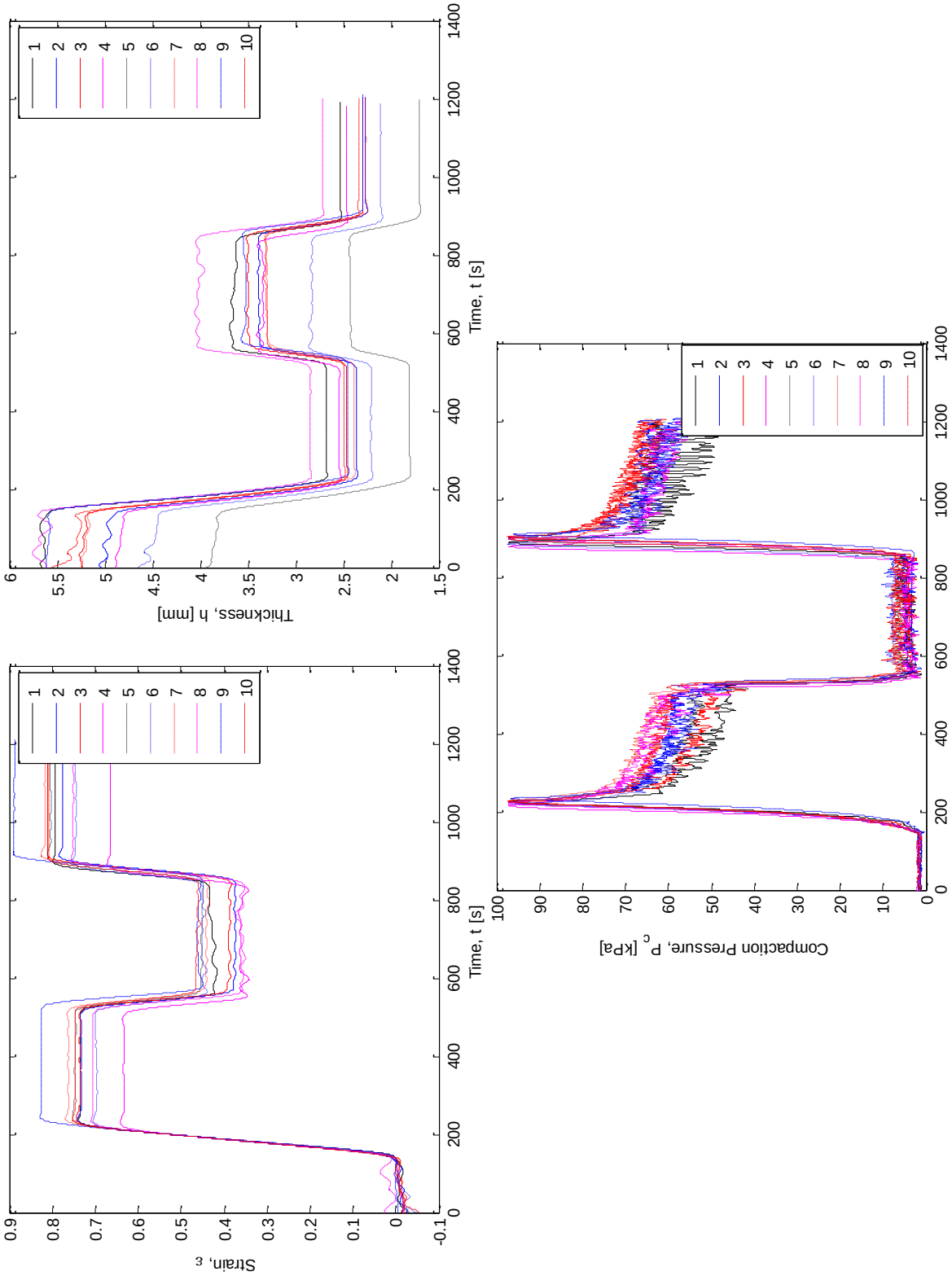

Figure 3.2. Experimental results for 8R; $d\varepsilon/dt = 0.01\ s^{-1}$; $P_{relaxation} = 1$ kPa

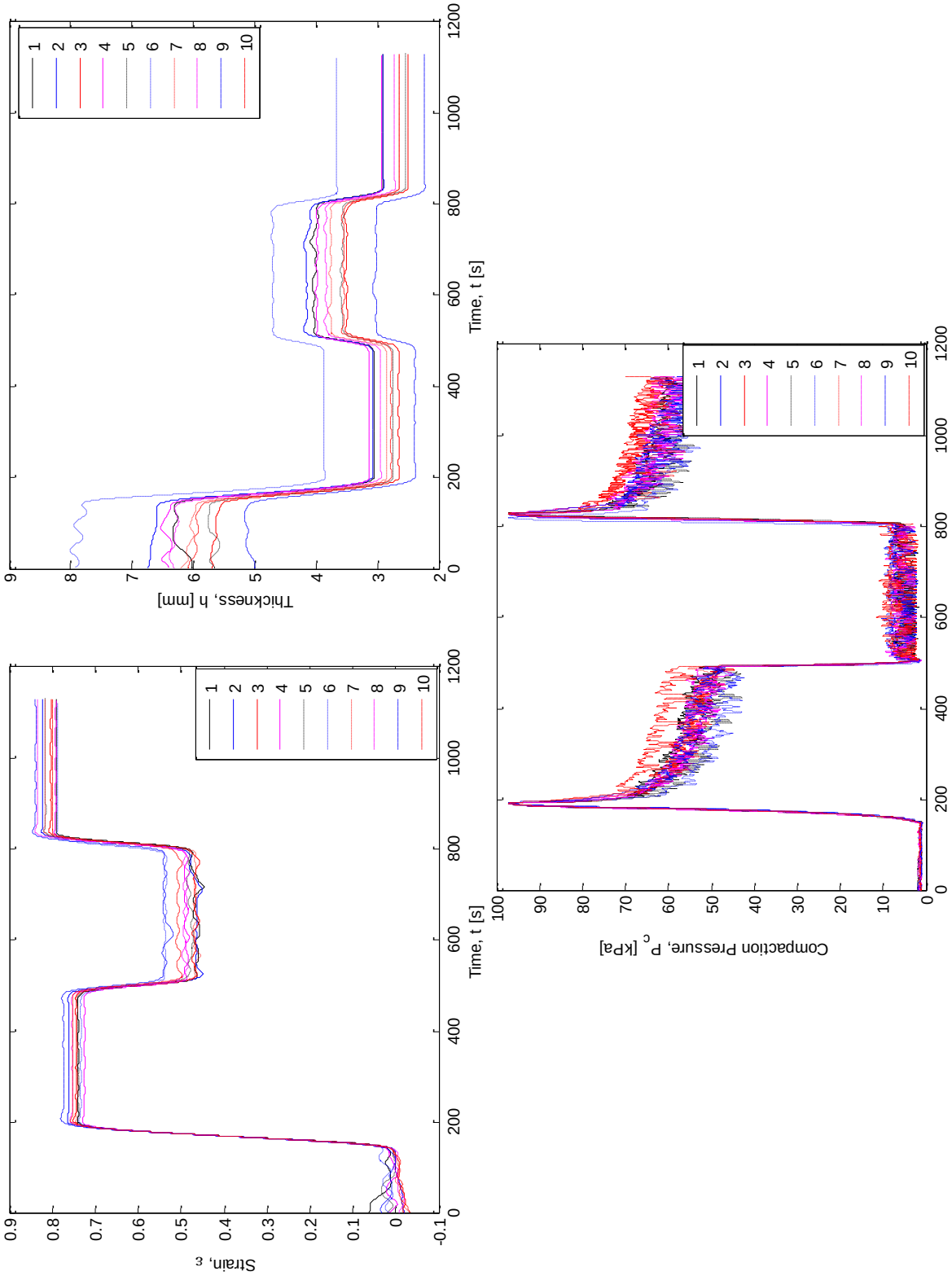

Figure 3.3. Experimental results for 8R; $d\varepsilon/dt = 0.02\ s^{-1}$; $P_{relaxation} = 1$ kPa

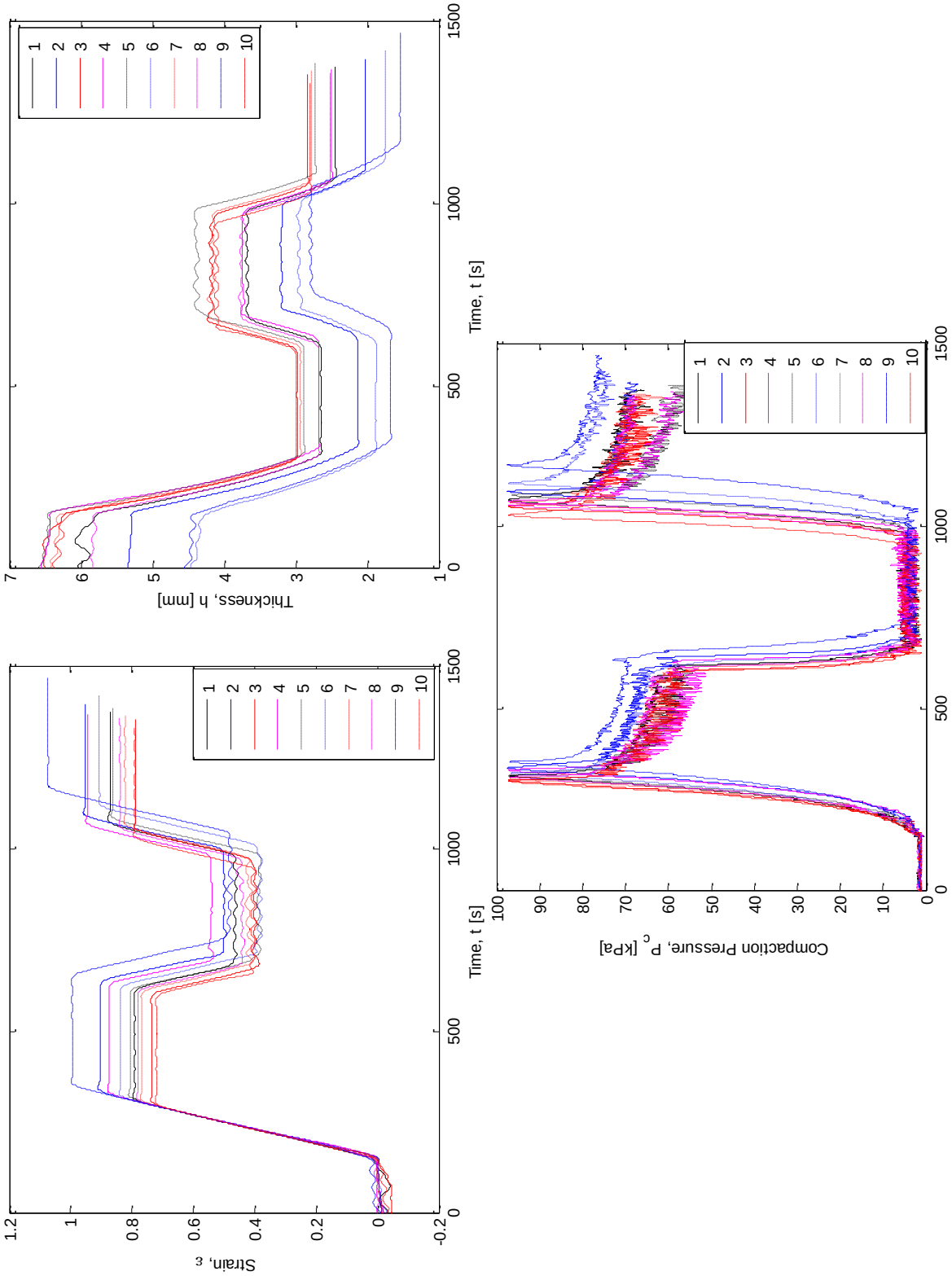

Figure 3.4. Experimental results for 8R; $d\varepsilon/dt = 0.005\ s^{-1}$; $P_{relaxation} = 1$ kPa

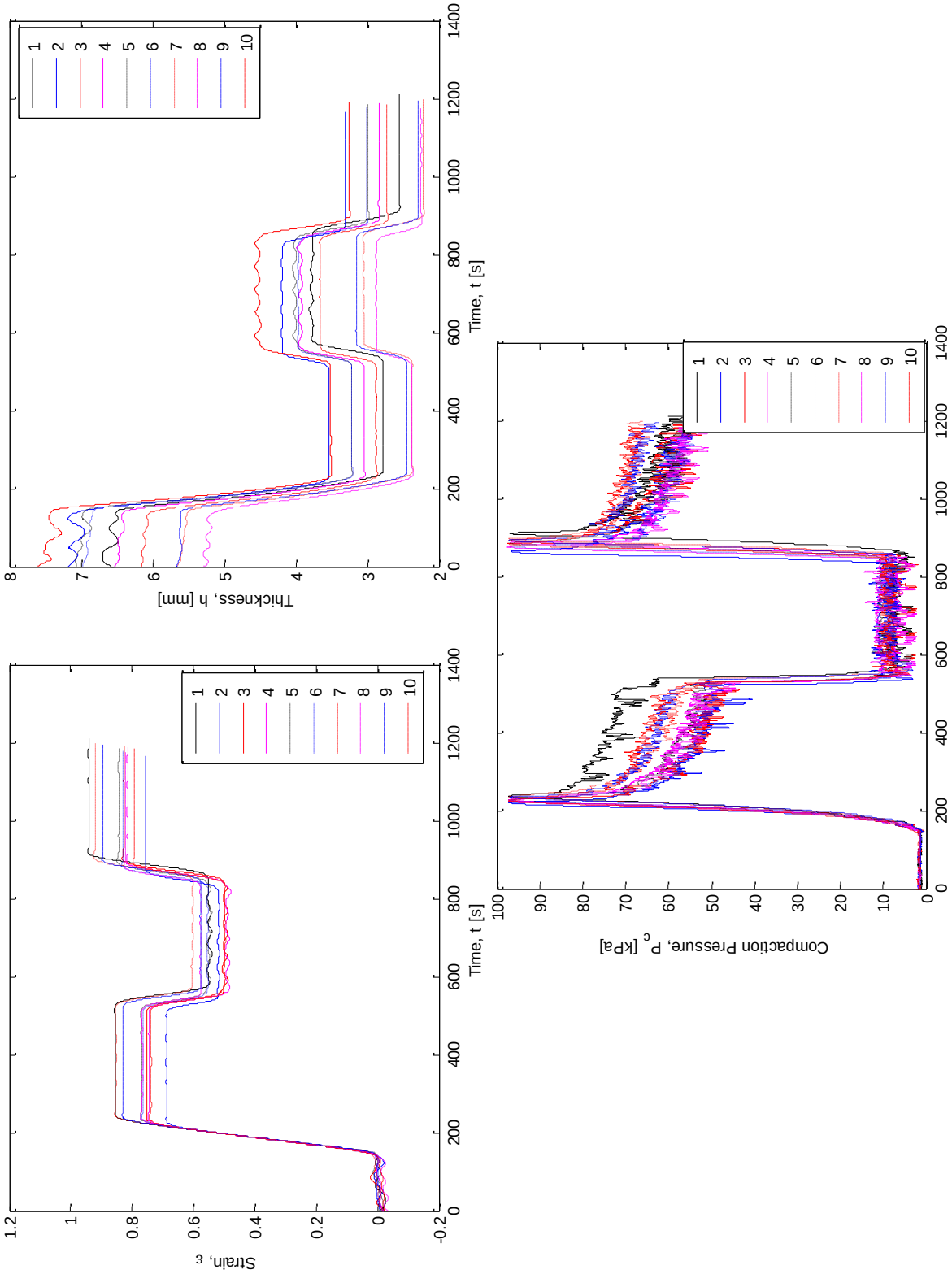

Figure 3.5. Experimental results for 8R; $d\varepsilon/dt = 0.01\ s^{-1}$; $P_{relaxation} = 5$ kPa

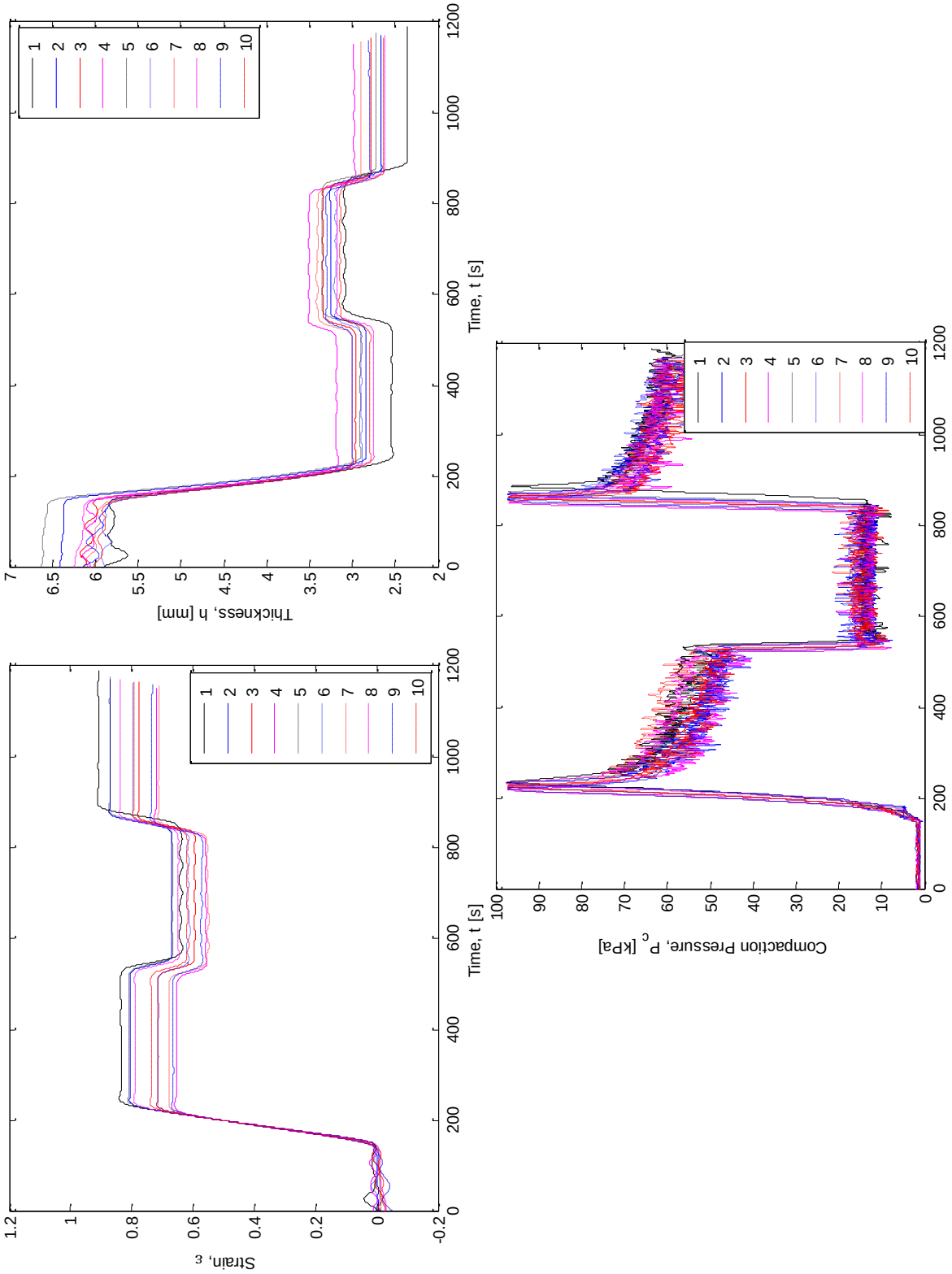

Figure 3.6. Experimental results for 8R; $d\varepsilon/dt = 0.01\ s^{-1}$; $P_{relaxation} = 10$ kPa

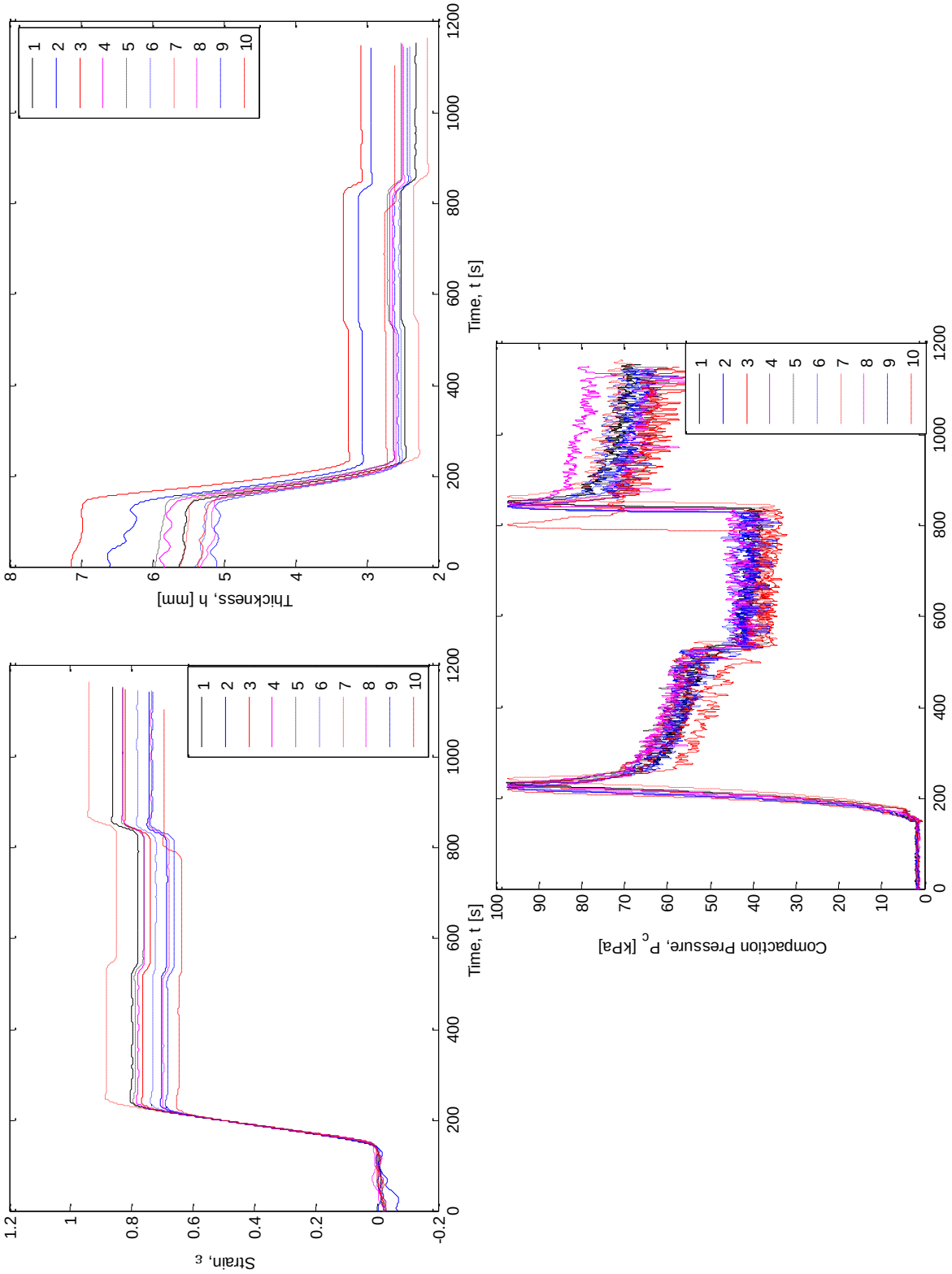

Figure 3.7. Experimental results for 8R; $d\varepsilon/dt = 0.01\ s^{-1}$; $P_{relaxation} = 40$ kPa

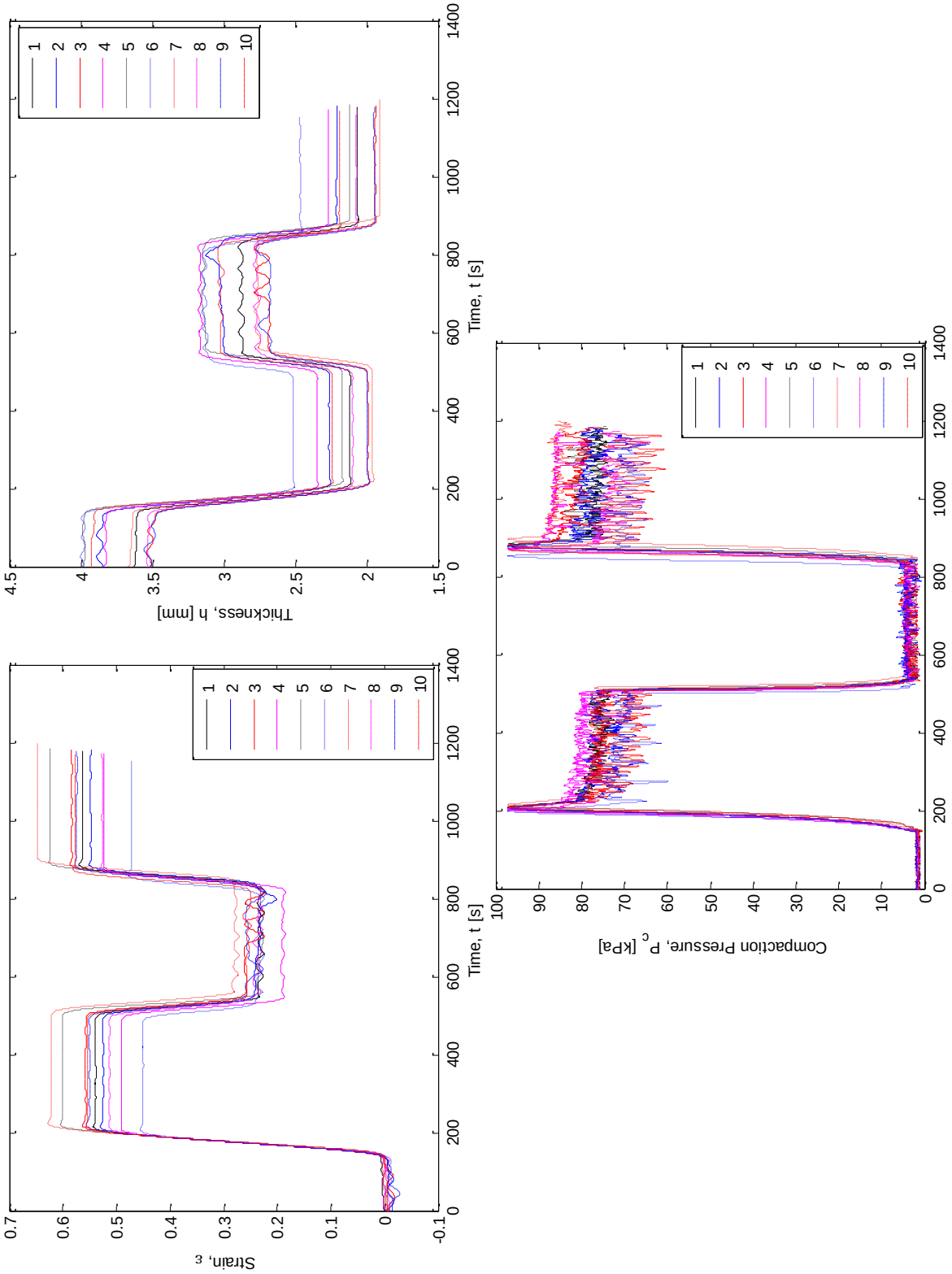

Figure 3.8. Experimental results for 8W; $d\varepsilon/dt = 0.01\ s^{-1}$; $P_{relaxation} = 1$ kPa; no wetting

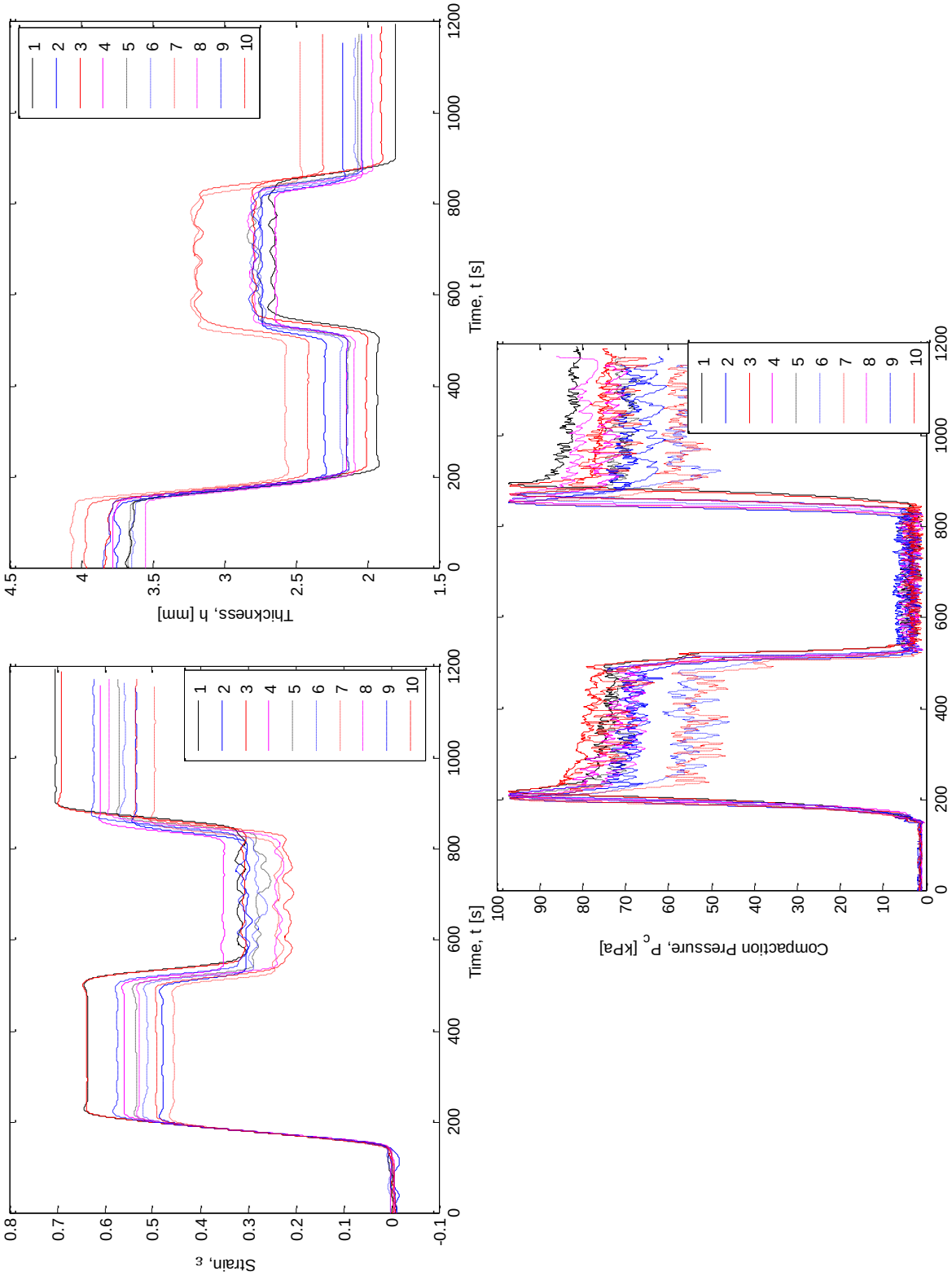

Figure 3.9. Experimental results for 8W; $d\varepsilon/dt = 0.01\ s^{-1}$; $P_{relaxation} = 1$ kPa

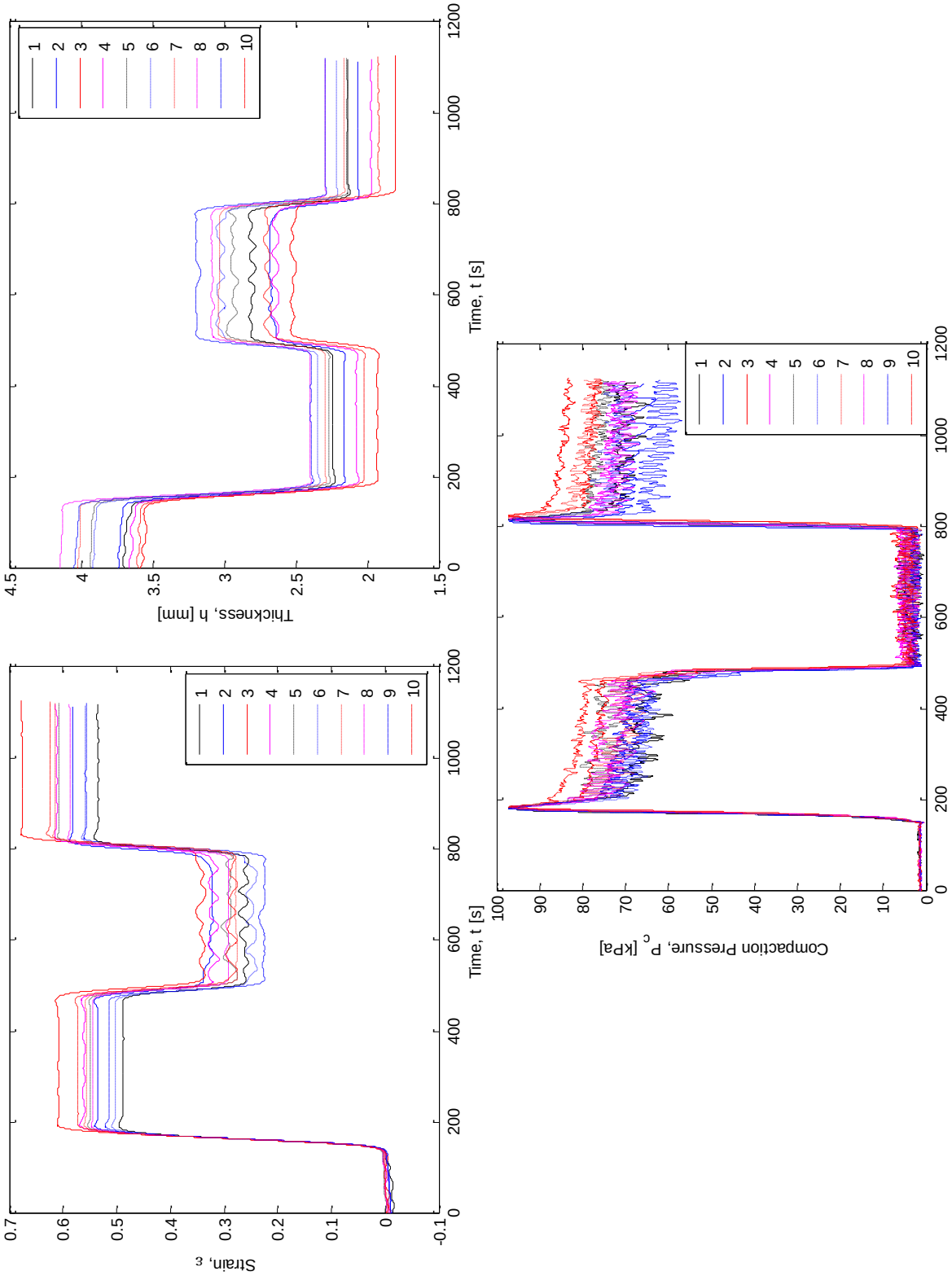

Figure 3.10. Experimental results for 8W; $d\varepsilon/dt = 0.02\ s^{-1}$; $P_{relaxation} = 1$ kPa

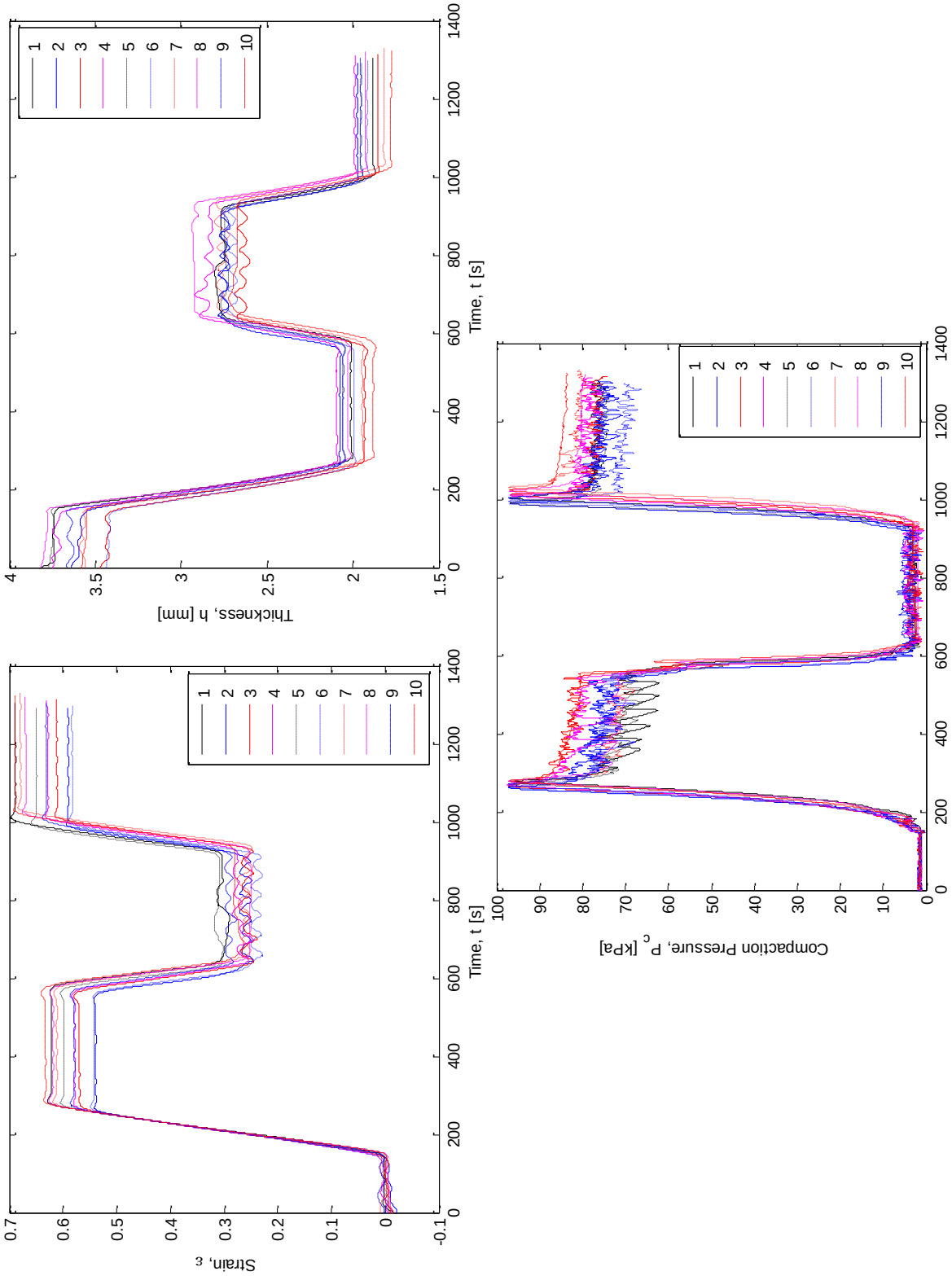

Figure 3.11. Experimental results for 8W; $d\varepsilon/dt = 0.005\ s^{-1}$; $P_{relaxation} = 1$ kPa

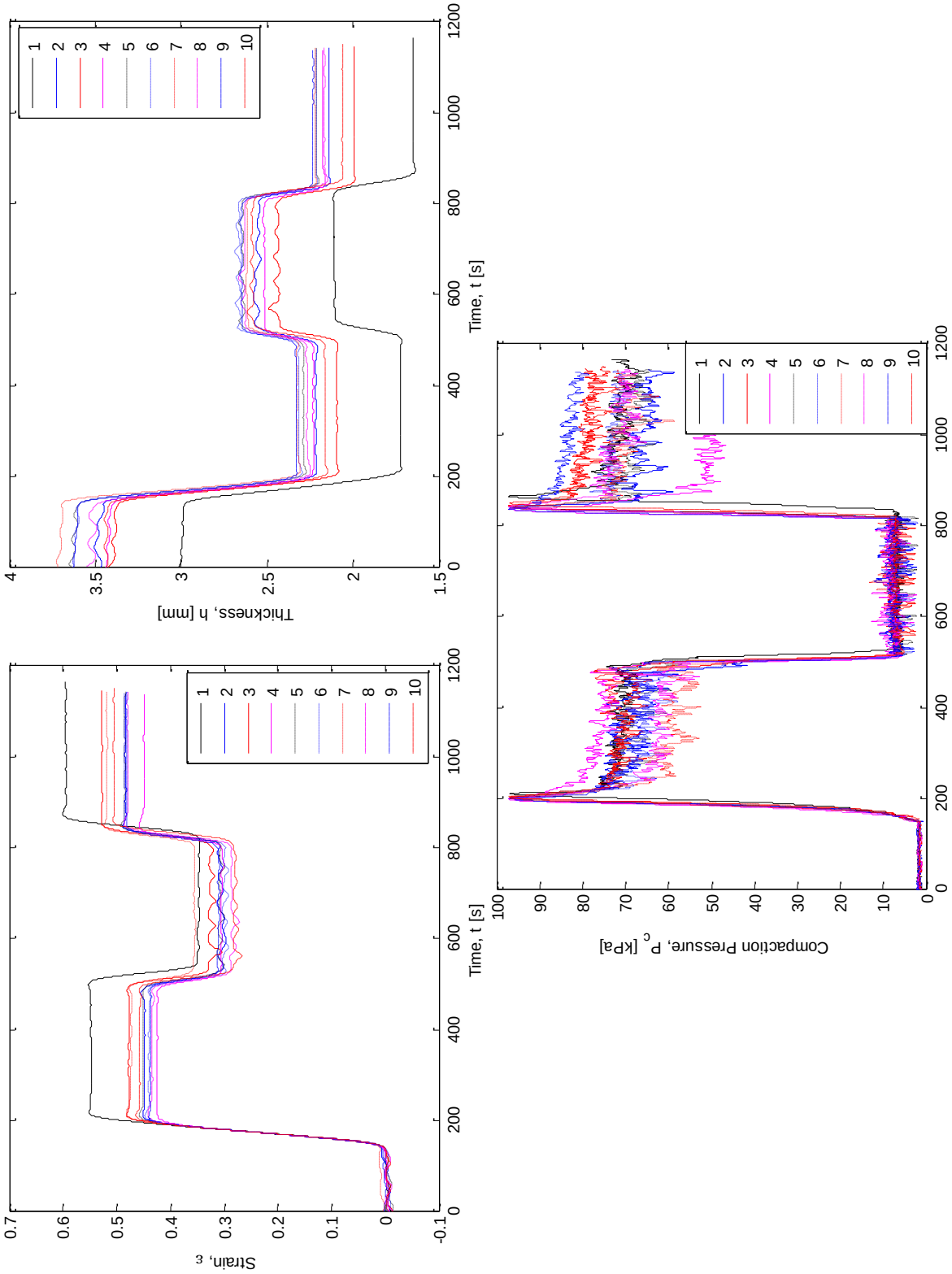

Figure 3.12. Experimental results for 8W; $d\varepsilon/dt = 0.01\ s^{-1}$; $P_{relaxation} = 5$ kPa

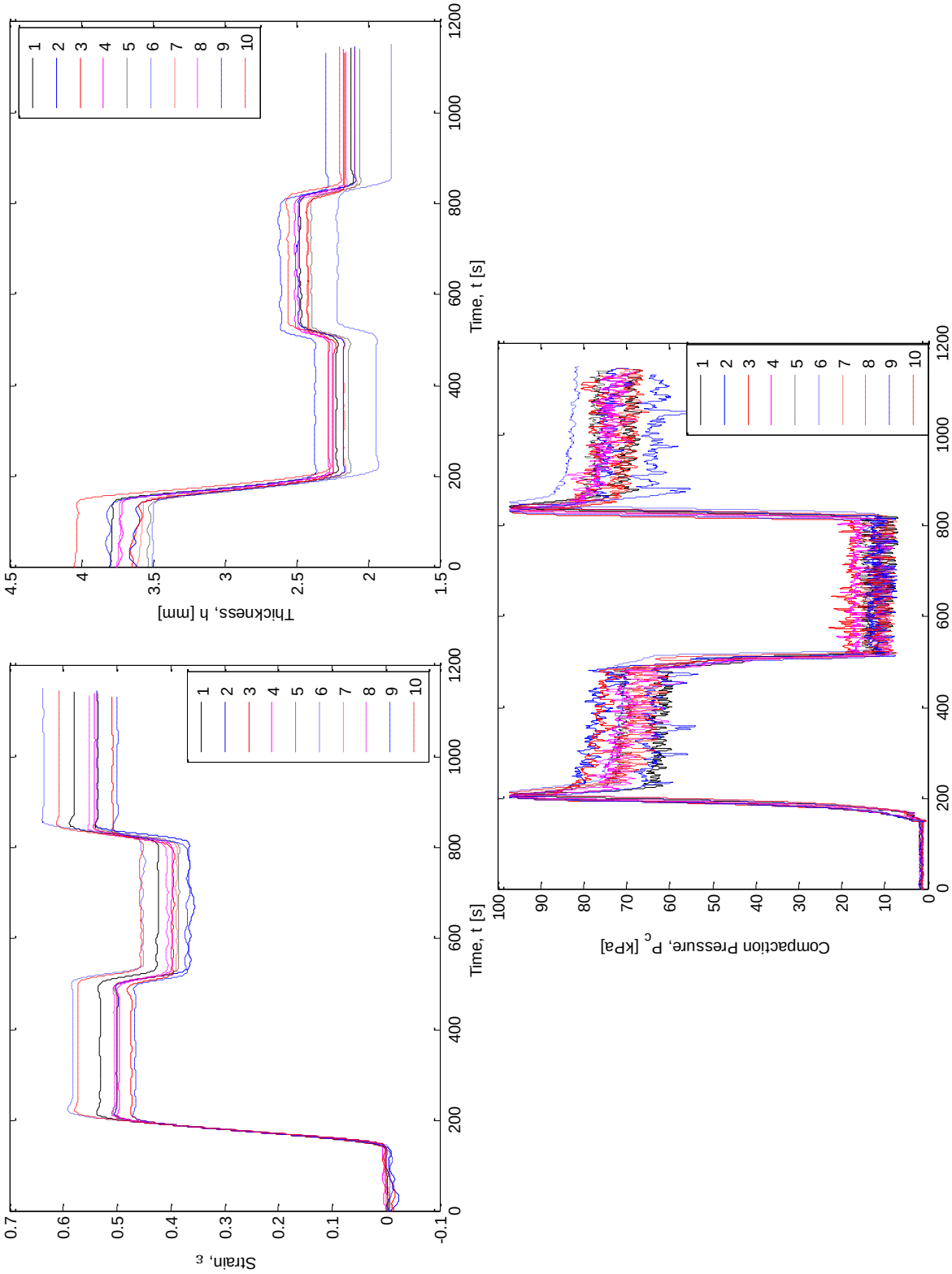

Figure 3.13. Experimental results for 8W; $d\varepsilon/dt = 0.01\ s^{-1}$; $P_{relaxation} = 10$ kPa

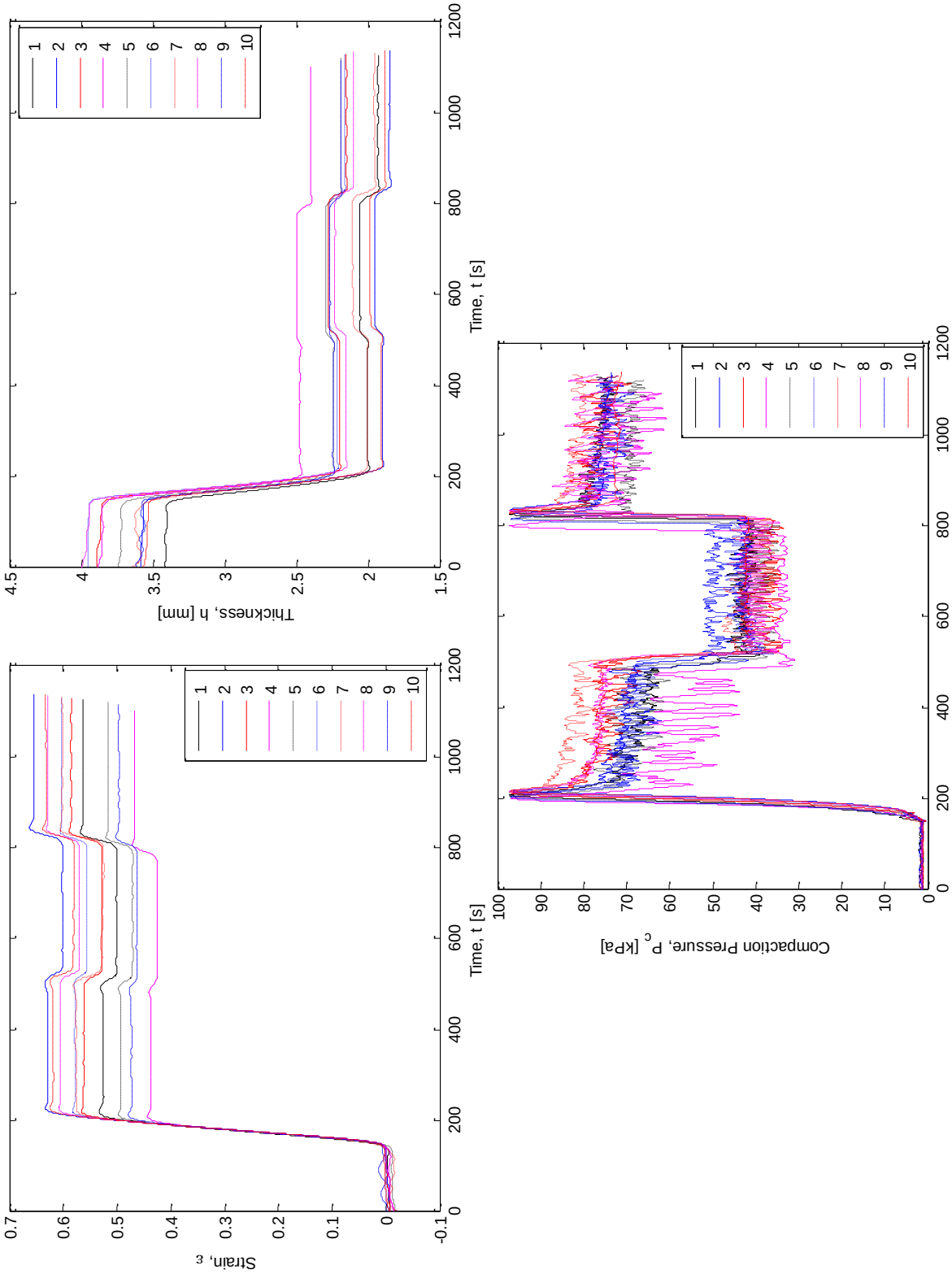

Figure 3.14. Experimental results for 8W; $d\varepsilon/dt = 0.01\ s^{-1}$; $P_{relaxation} = 40$ kPa

In this study, the strain rate controlled experiments are performed using a PID controller that controls strain/thickness and measures the compaction pressure as explained in the previous sections. Therefore, depending on the PID constants selected, the system may show oscillatory behavior especially for the pressure data (compaction pressure data has peaks and dips while trying to set the desired strain value). To reduce the oscillations of the experimental data, a low-pass filter is generated and applied to the data. The filtering parameters are chosen in a manner such that the oscillations are minimized and the experimental behavior of the system is not affected so that the compaction characterization of the specimen is clearly understood. The filtering is done by using the built-in functions of Matlab. For the strain and thickness data, "filtfilt" function is used as the low-pass filter. Function parameters are chosen as a = 2 (the order of the low-pass analog Bessel filter) and b = 0.01 (the frequency of the low-pass filter) while filtering strain and thickness data of the experiments. As a sample, the raw and filtered data of one experiment (Experiment 1 for random fabric under nominal characterization parameters) are seen in Figures 3.15 and 3.16.

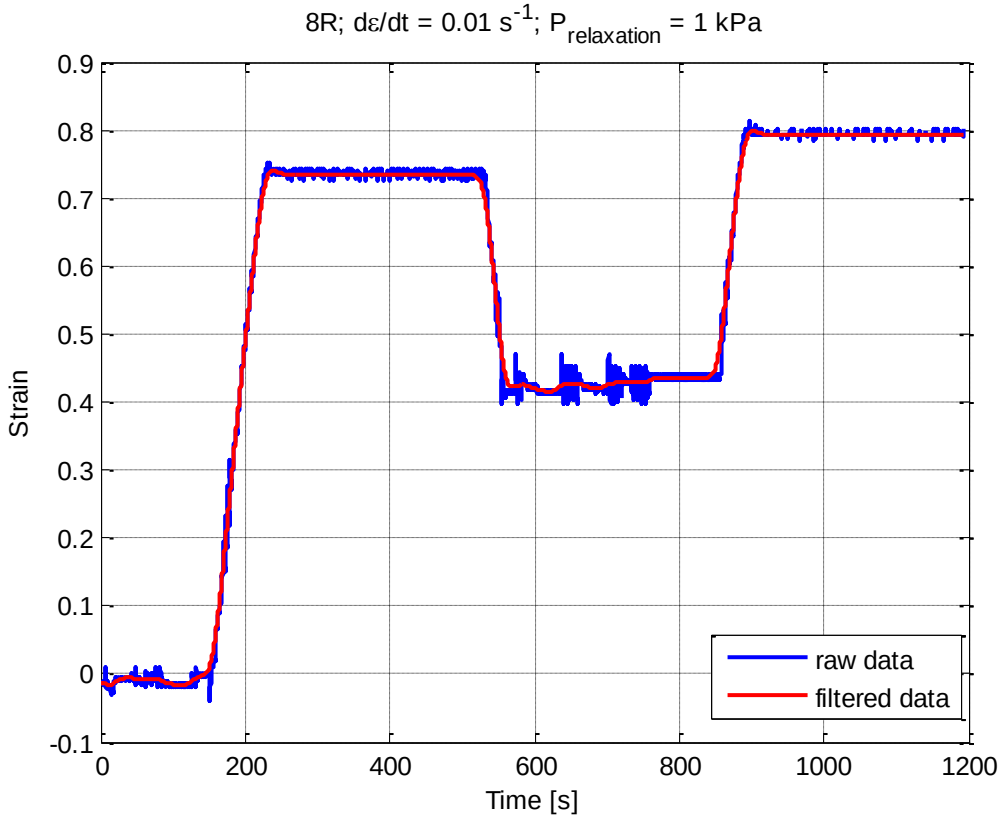

Figure 3.15. The filtered and the raw strain data of experiment 1 for random fabric under nominal characterization parameters

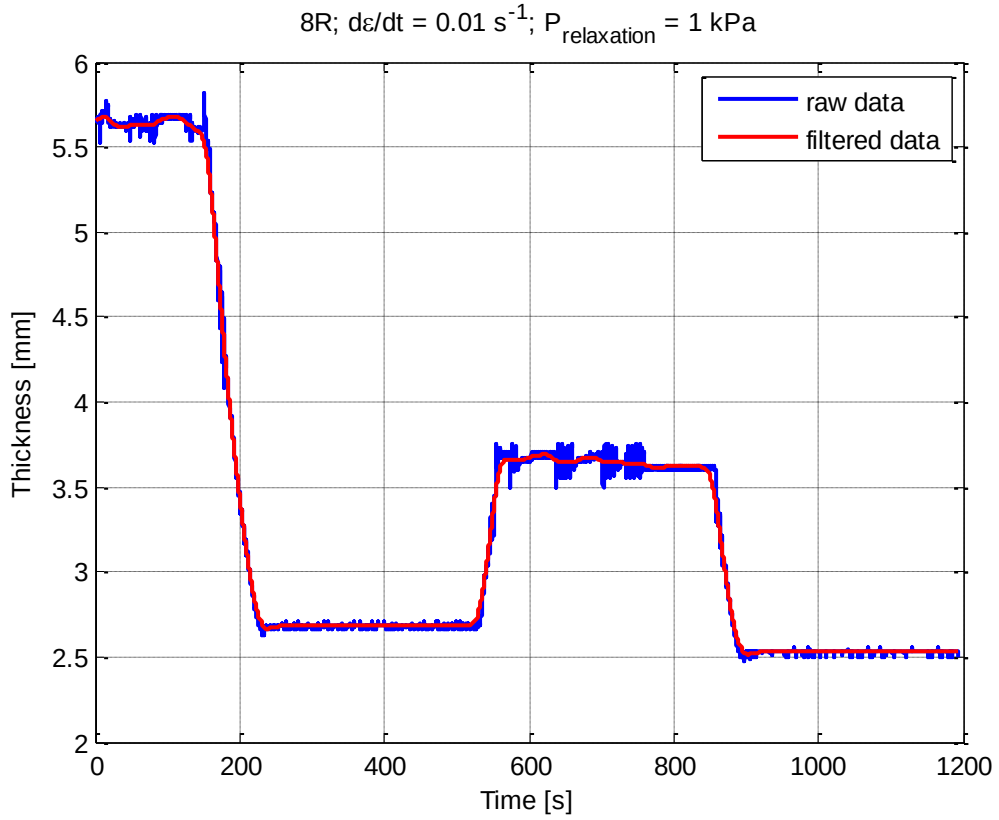

Figure 3.16. The filtered and the raw thickness data of experiment 1 for random fabric under nominal characterization parameters

For the filtering of pressure data, another Matlab function (“smooth”) is used, because the previous filtering method does not filter the pressure data as well as it filters the strain and the thickness data. Two case studies of filtering the pressure data with the previous method are seen in Figures 3.17 and 3.18. For the case seen in Figure 3.17, the oscillations are not minimized well compared to the case seen in Figure 3.18. As it can be seen in the figures, the pressure data has a peak value at the end of the loading stage. If the filtering is strict, this peak value is recognized as oscillation, and disappears as seen in Figure 3.18. For this reason, “smooth” function of Matlab is used for the filtering of the pressure data. This filtering function causes less oscillation without losing the peak value as seen in Figure 3.19.

In this study, strain rate controlled experiments are performed. Pressure rate controlled experiments are performed and the comparison of the two types are given in Yenilmez’s thesis [4].

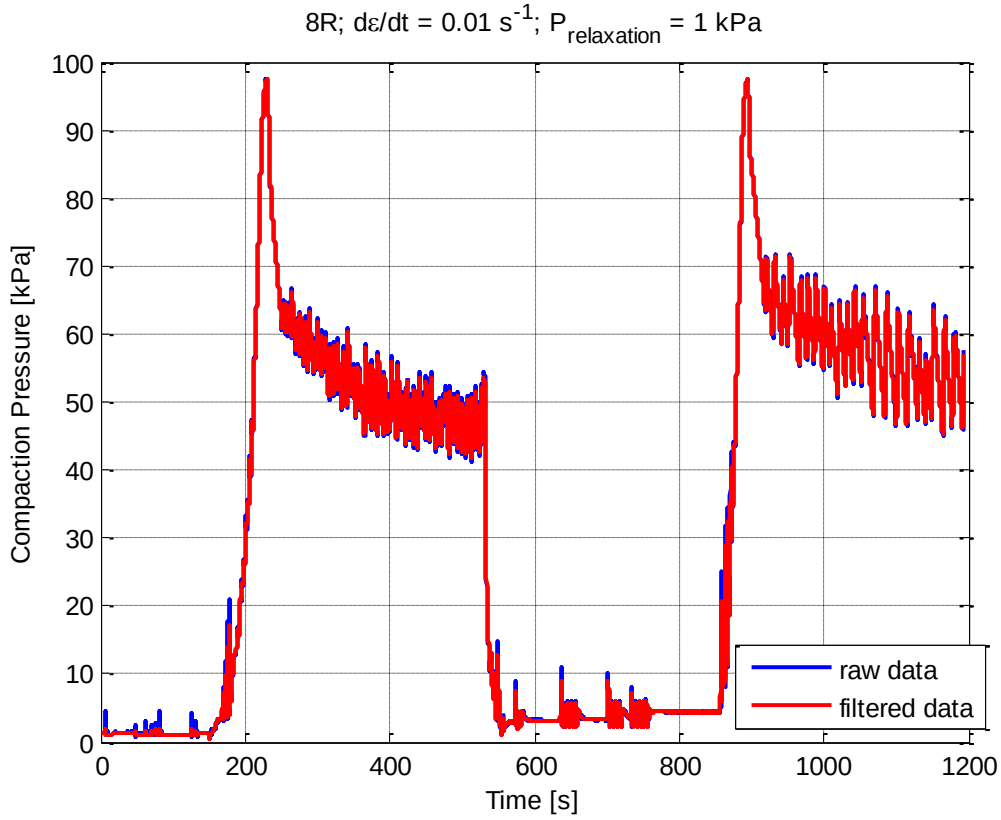

Figure 3.17. Case A (a = 2; b = 0.5): The filtered and the raw pressure data of experiment 1 for random fabric under nominal characterization parameters

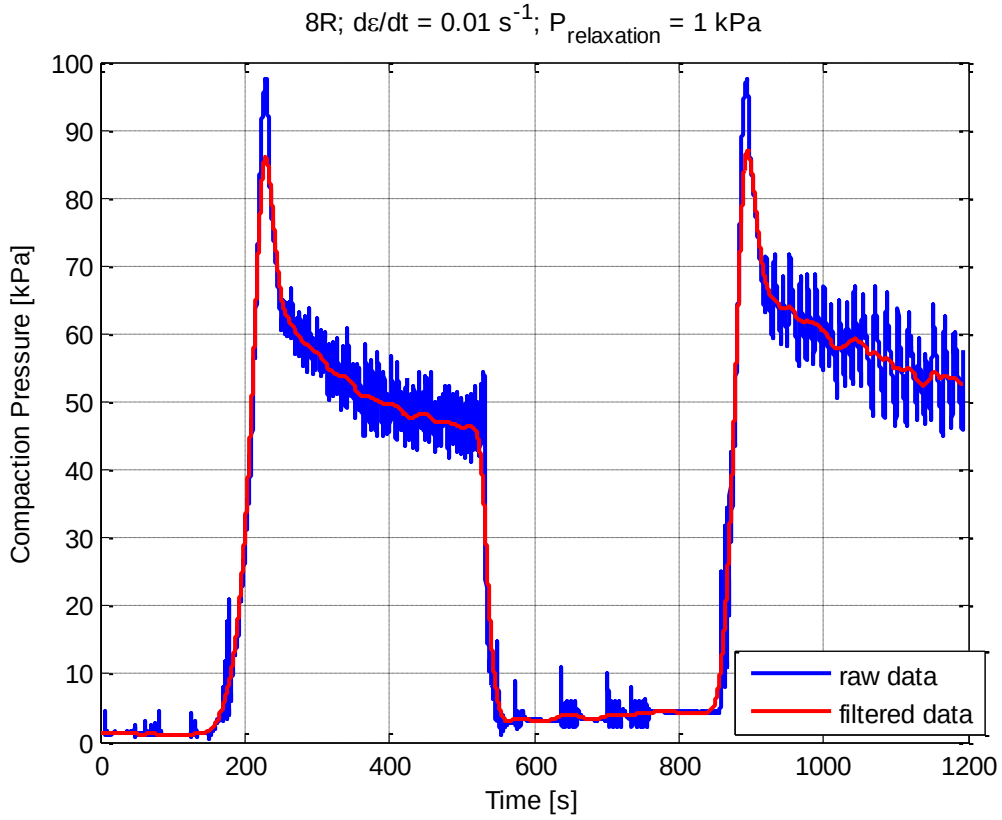

Figure 3.18. Case B (a = 2; b = 0.01): The filtered and the raw pressure data of experiment 1 for random fabric under nominal characterization parameters

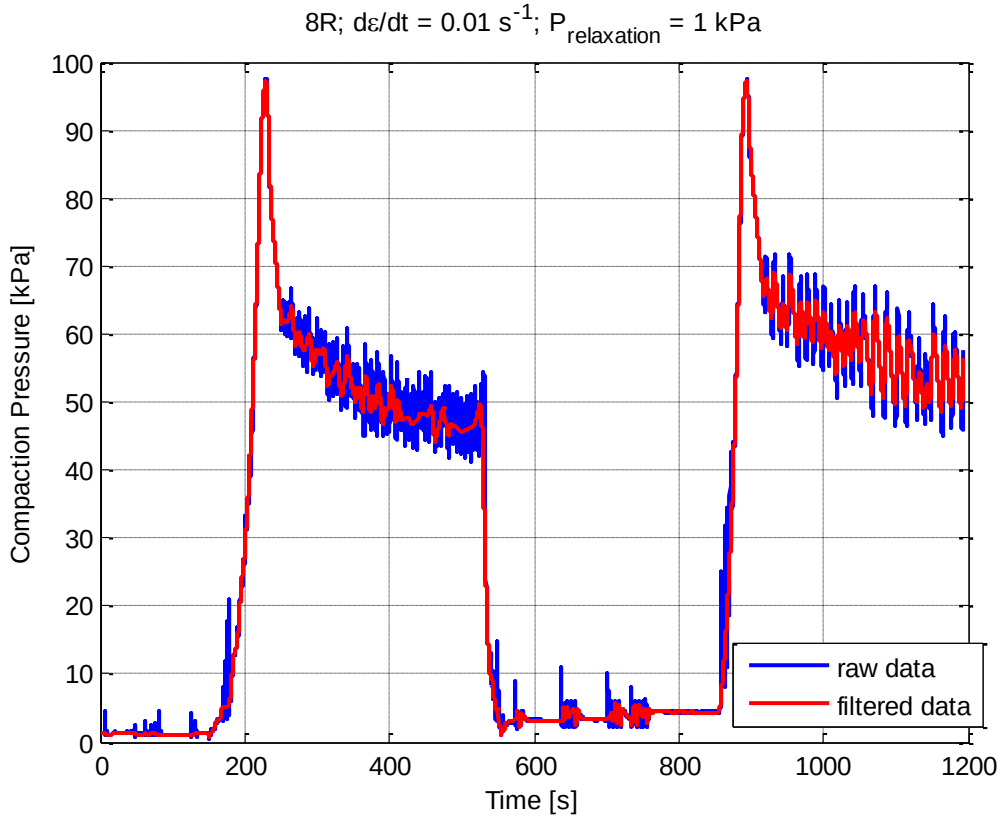

Figure 3.19. Case C (using the "smooth" function): The filtered and the raw pressure data of Experiment 1 for random fabric under nominal characterization parameters

Chapter 4

MODEL FITTING

The mathematical model suggested in Yenilmez's thesis [4] is analogically similar to standard linear solid model with the exception that the elastic component is taken non-linear here.

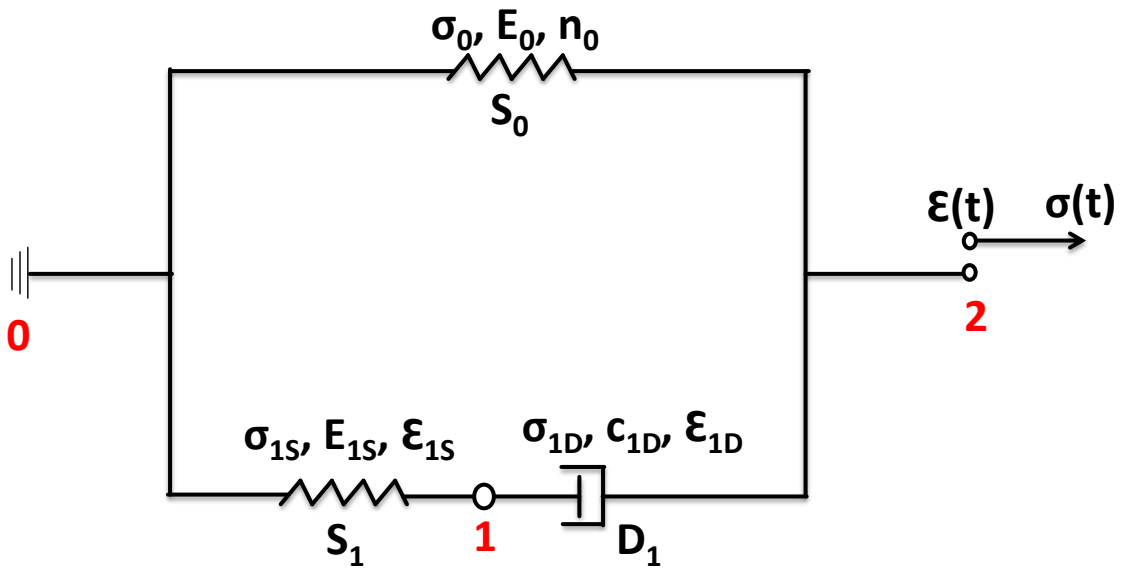

Figure 4.1. Schematic of the mathematical model

Constitutive equations of the elements are given below

Spring 0, S_0 : $\sigma_0 = E_0 \varepsilon^{n_0}, \quad \varepsilon \geq 0$ (4)

Spring 1, S_1 : $\sigma_{1S} = E_1 \varepsilon_{1S}$ (5)

Damper 1, D_1 : $\sigma_{1D} = c_1 \dot{\varepsilon}_{1D}$ (6)

Equilibrium at nodes 1 and 2 gives

$$\sigma_{1S} = \sigma_{1D} = \sigma_1 \tag{7}$$

$$\sigma_1 + \sigma_0 = \sigma \tag{8}$$

Geometric constraint gives

$$\varepsilon_{1S} + \varepsilon_{1D} = \varepsilon \tag{9}$$

By differentiating Equations (5) and (9) and combining them with Equation (6) gives

$$\dot{\varepsilon}_{1S} + \dot{\varepsilon}_{1D} = \dot{\varepsilon} \tag{10}$$

$$\dot{\sigma}_{1S} = E_1 \dot{\varepsilon}_{1S} \tag{11}$$

$$\frac{\dot{\sigma}_{1S}}{E_1} + \frac{\sigma_{1D}}{c_1} = \dot{\varepsilon} \tag{12}$$

Recall Equation (7);

$$\frac{\dot{\sigma}_1}{E_1} + \frac{\sigma_1}{c_1} = \dot{\varepsilon} \tag{13}$$

Replace σ_1 with $\sigma - \sigma_0$ using Equation (8);

$$\frac{\dot{\sigma}-\dot{\sigma}_0}{E_1}+\frac{\sigma-\sigma_0}{c_1}=\dot{\varepsilon} \tag{14}$$

Using Equation (4) and its derivative;

$$\frac{\dot{\sigma}-E_0 n_0 \varepsilon^{n_0-1}\dot{\varepsilon}}{E_1}+\frac{\sigma-E_0\varepsilon^{n_0}}{c_1}=\dot{\varepsilon} \tag{15}$$

Leaving $\dot{\varepsilon}$ on one side

$$\dot{\varepsilon}=\frac{\dot{\sigma}+\frac{E_1}{c_1}\left(\sigma-E_0\varepsilon^{n_0}\right)}{E_1+E_0 n_0 \varepsilon^{n_0-1}} \tag{16}$$

To solve for σ, we can rearrange it as

$$\dot{\sigma}=\dot{\varepsilon}\left(E_1+E_0 n_0 \varepsilon^{n_0-1}\right)-\frac{E_1}{c_1}\left(\sigma-E_0\varepsilon^{n_0}\right) \tag{17}$$

Note that ε is controlled, and it always satisfies $\varepsilon \geq 0$. On the other hand, $\sigma \leq 0$ physically since we can only apply compaction load but not tension. To include this behavior in the formula, one can write the equation as;

$$\dot{\sigma}_A=\begin{cases} 0 & \text{for } \sigma<0 \text{ and } \dot{\sigma}<0 \\ \dot{\sigma} & \text{otherwise} \end{cases} \tag{18}$$

where $\dot{\sigma}_A$ is the rate of actual stress applied on the specimen.

The experimental results indicated in the previous section are fitted to Equation (16). Fitting results and model parameters are shown in Figures 4.2 - 4.15. Tables 4.1 and 4.2 indicate the list of figures and model parameters.

Table 4.1. The list of figures showing model fits on experimental results for random fabric with different experimental procedures such as varying dε/dt and $P_{relaxation}$ values, and wetting condition

Random Fabric	**dε/dt**	**$P_{relaxation}$**	**Wetting**
Figure 4.2	0.01 s^{-1}	1 kPa	✘
Figure 4.3	0.01 s^{-1}	1 kPa	✓
Figure 4.4	0.02 s^{-1}	1 kPa	✓
Figure 4.5	0.005 s^{-1}	1 kPa	✓
Figure 4.6	0.01 s^{-1}	5 kPa	✓
Figure 4.7	0.01 s^{-1}	10 kPa	✓
Figure 4.8	0.01 s^{-1}	40 kPa	✓

Table 4.2. The list of figures showing model fits on experimental results for random fabric with different experimental procedures such as varying dε/dt and $P_{relaxation}$ values, and wetting condition

Woven Fabric	**dε/dt**	**$P_{relaxation}$**	**Wetting**
Figure 4.9	0.01 s^{-1}	1 kPa	✘
Figure 4.10	0.01 s^{-1}	1 kPa	✓
Figure 4.11	0.02 s^{-1}	1 kPa	✓
Figure 4.12	0.005 s^{-1}	1 kPa	✓
Figure 4.13	0.01 s^{-1}	5 kPa	✓
Figure 4.14	0.01 s^{-1}	10 kPa	✓
Figure 4.15	0.01 s^{-1}	40 kPa	✓

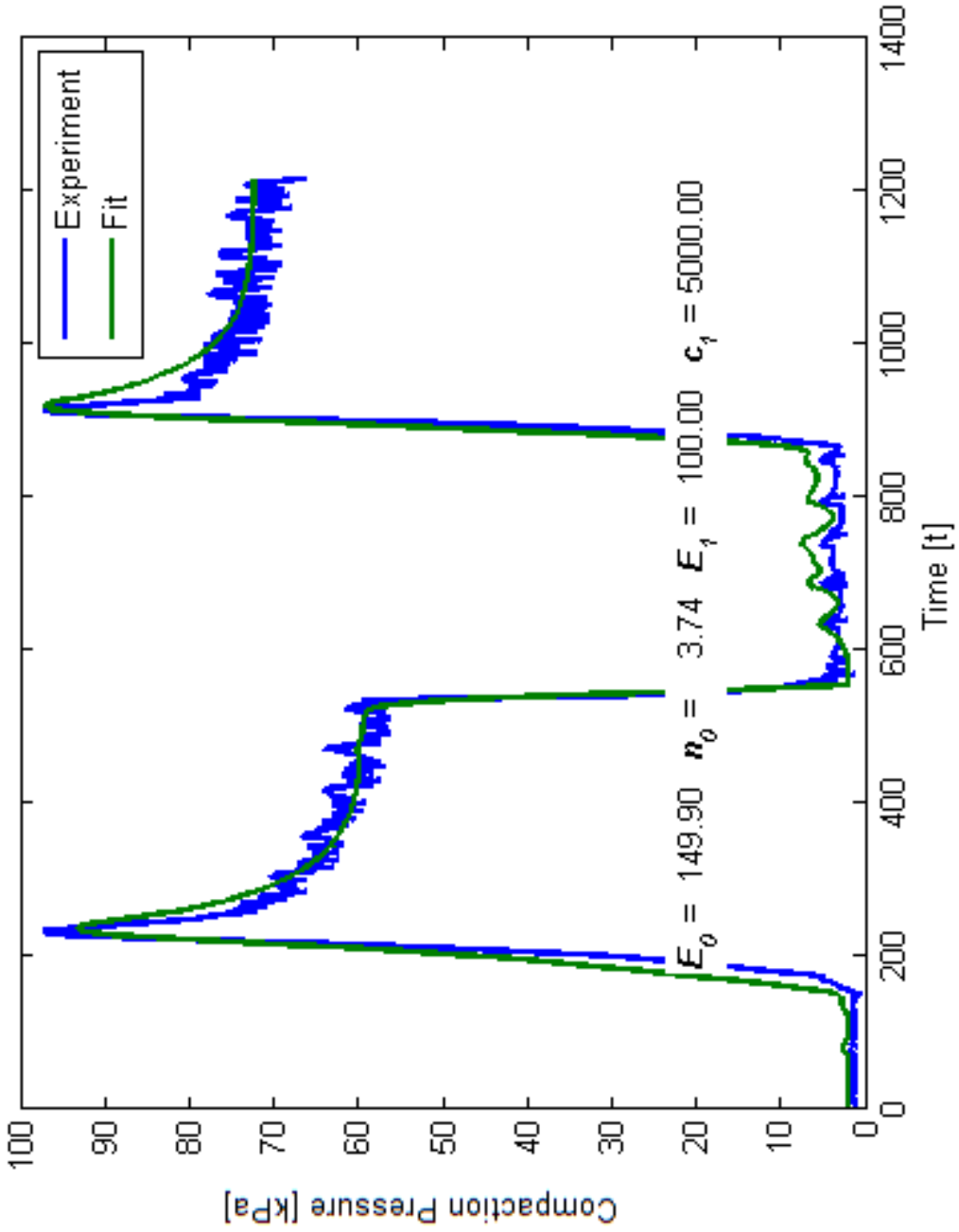

Figure 4.2. Model fits on experimental results for 8R; $d\varepsilon/dt = 0.01\ s^{-1}$; $P_{relaxation}$ = 1 kPa; no wetting

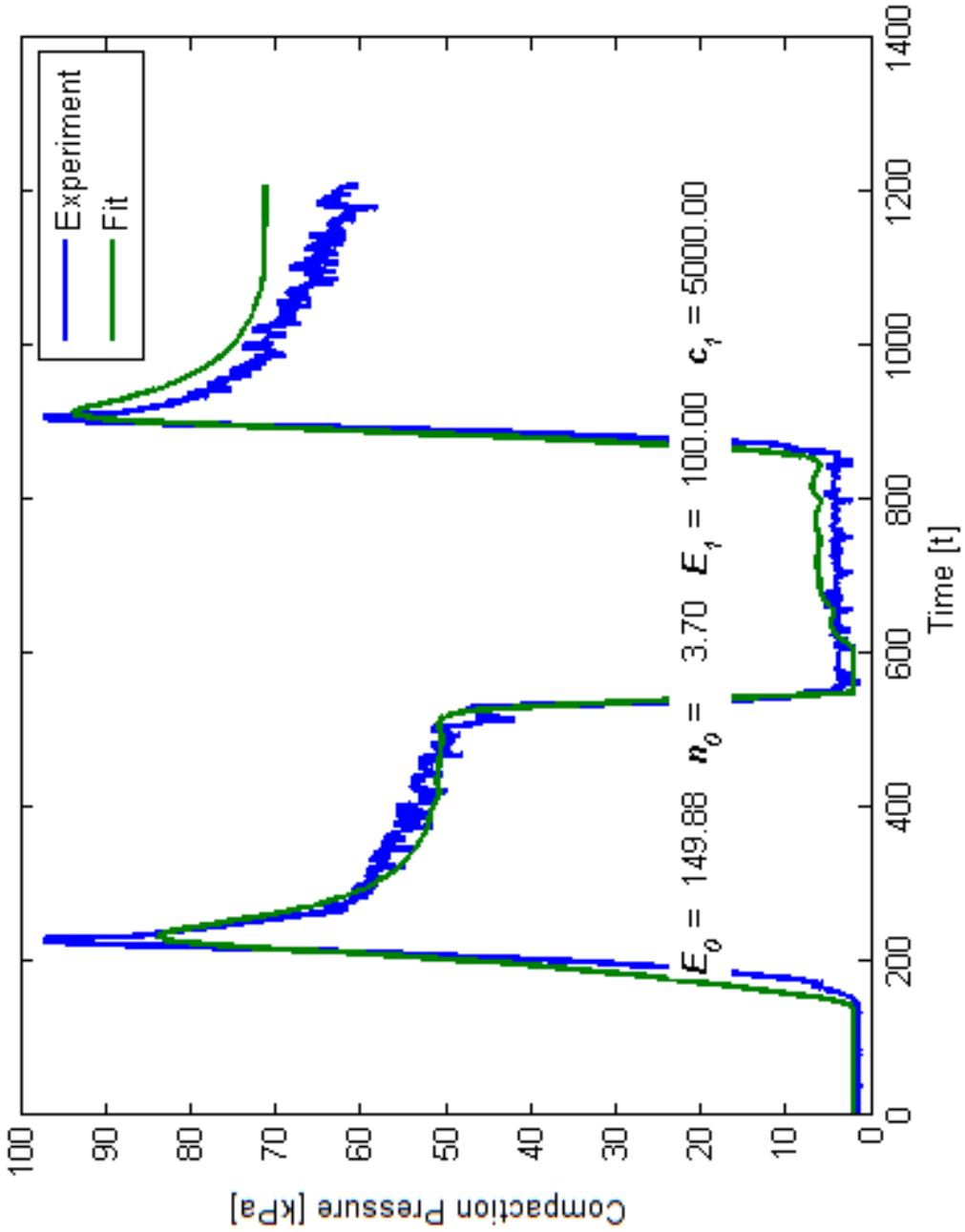

Figure 4.3. Model fits on experimental results for 8R; $d\varepsilon/dt = 0.01\ s^{-1}$; $P_{relaxation} = 1$ kPa

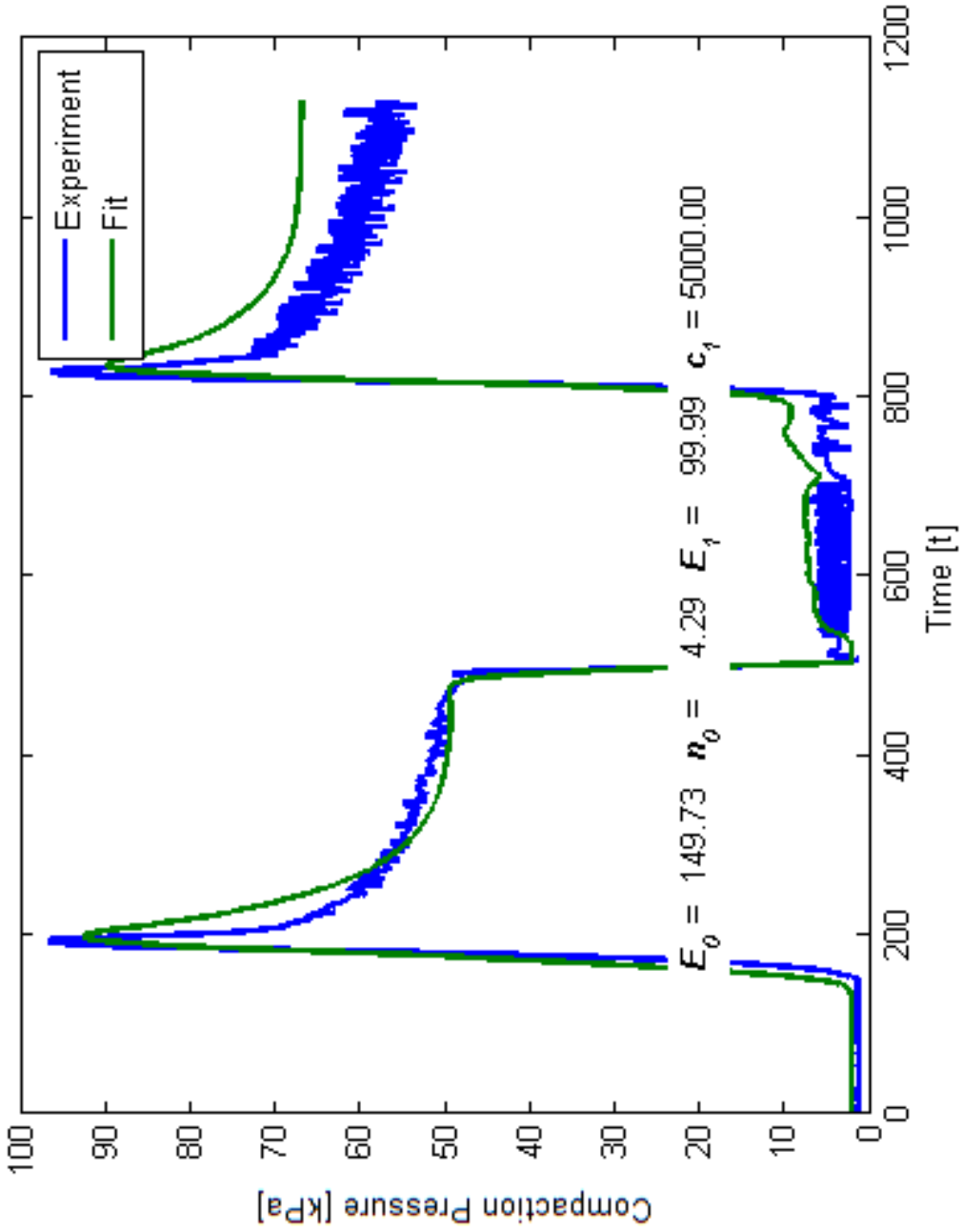

Figure 4.4. Model fits on experimental results for 8R; $d\varepsilon/dt = 0.02\ s^{-1}$; $P_{relaxation} = 1$ kPa

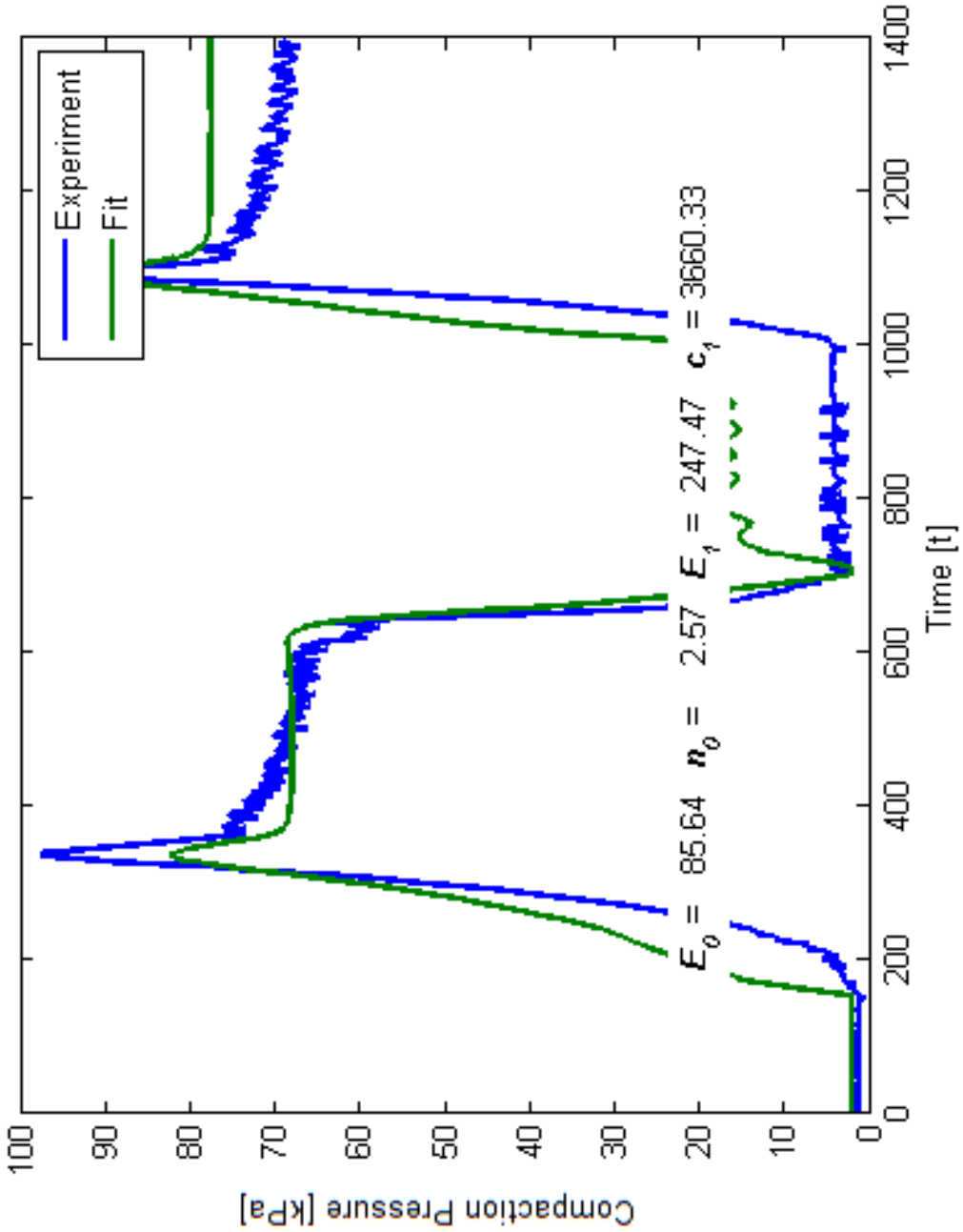

Figure 4.5. Model fits on experimental results for 8R; $d\varepsilon/dt = 0.005\ s^{-1}$; $P_{relaxation} = 1$ kPa

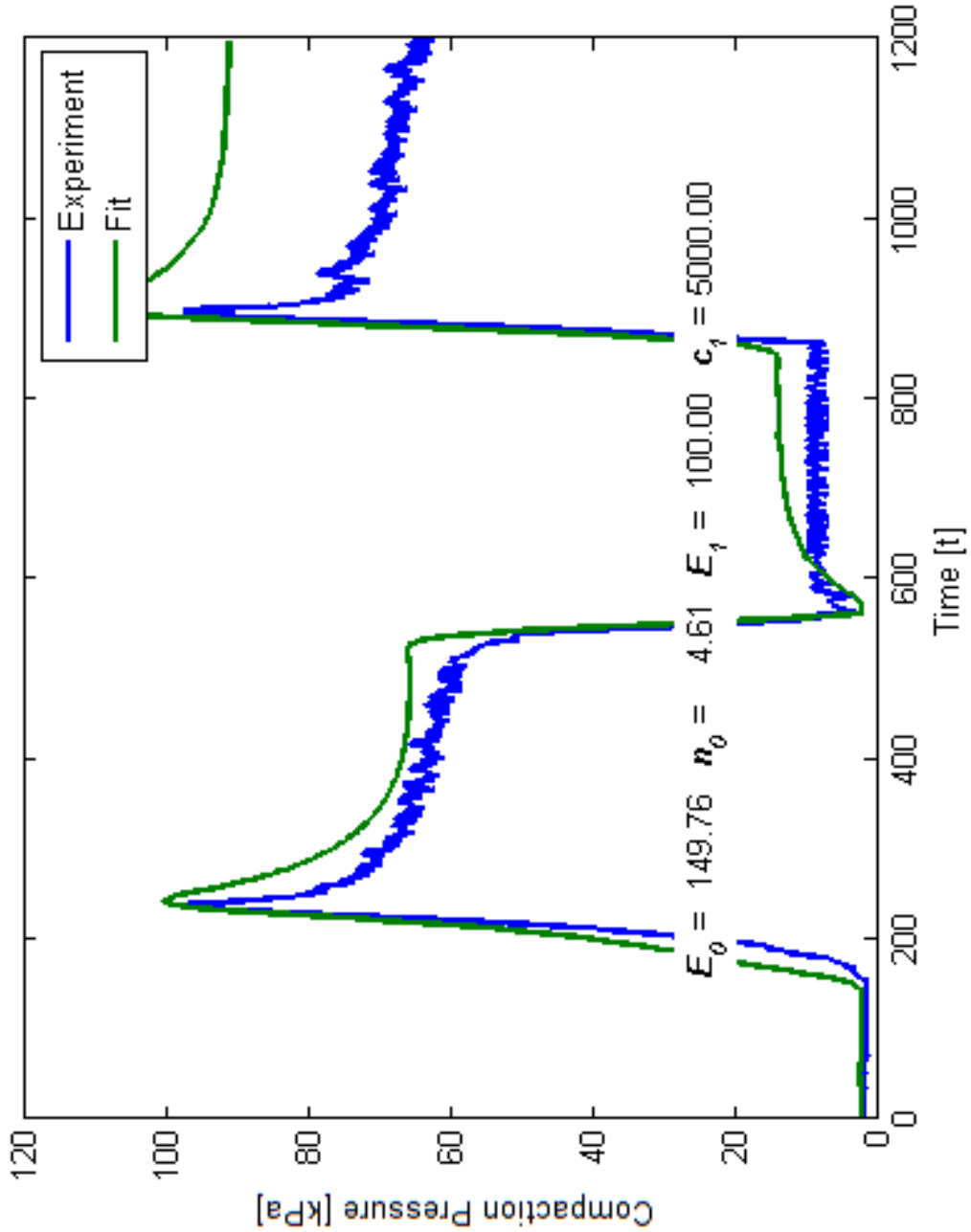

Figure 4.6. Model fits on experimental results for 8R; $d\varepsilon/dt = 0.01\ s^{-1}$; $P_{relaxation} = 5$ kPa

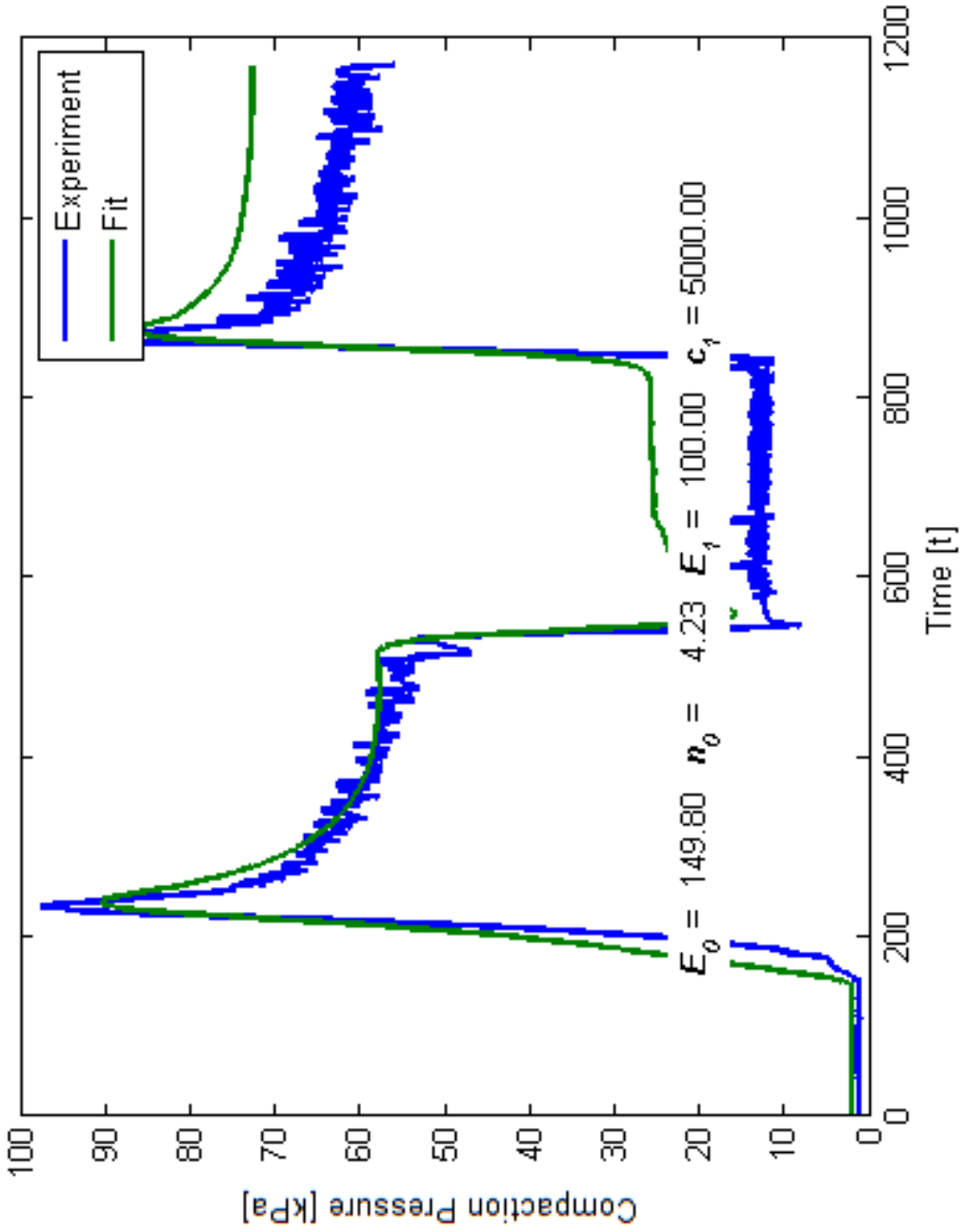

Figure 4.7. Model fits on experimental results for 8R; $d\varepsilon/dt = 0.01\ s^{-1}$; $P_{relaxation} = 10$ kPa

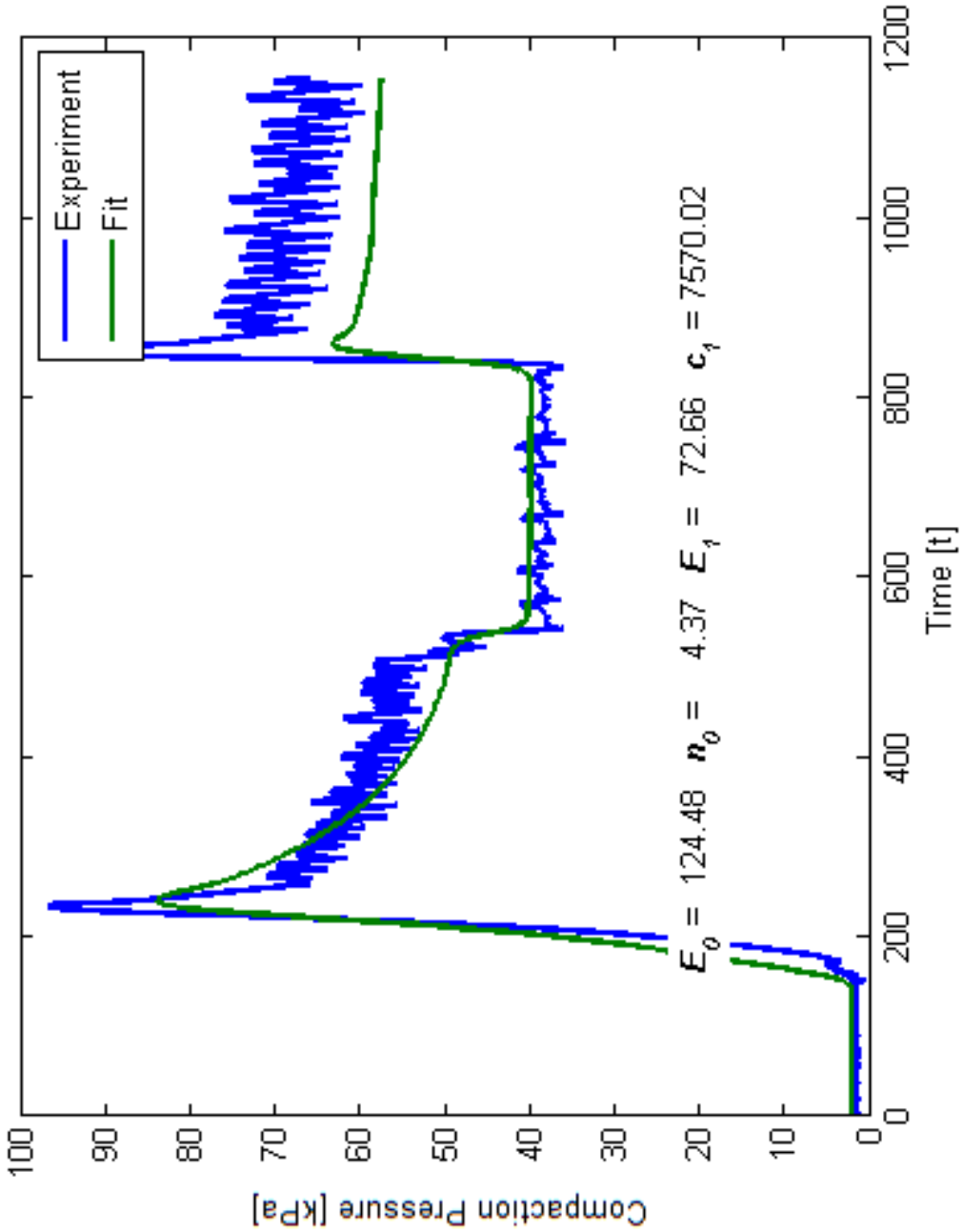

Figure 4.8. Model fits on experimental results for 8R; $d\varepsilon/dt = 0.01\ s^{-1}$; $P_{relaxation} = 40$ kPa

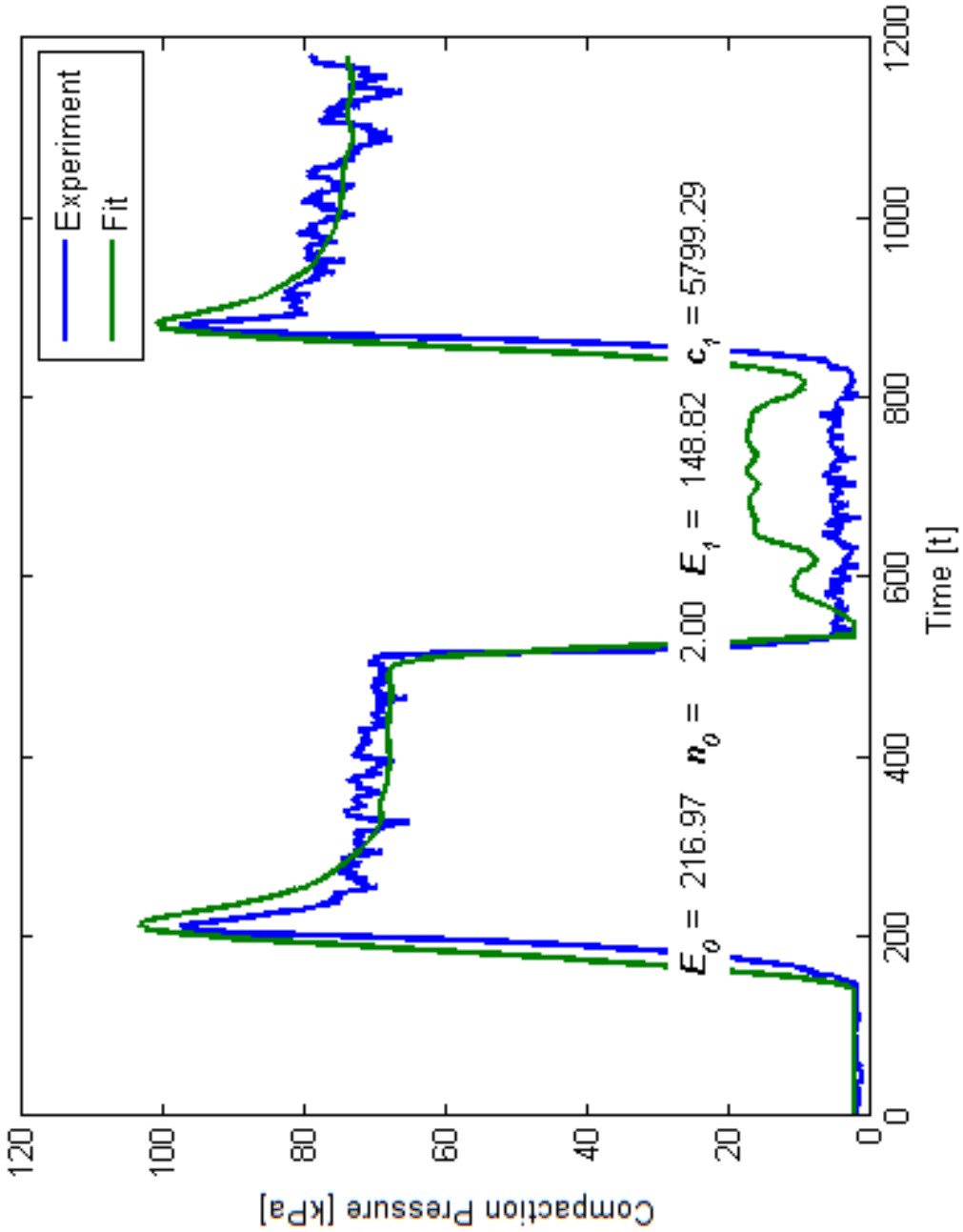

Figure 4.9. Model fits on experimental results for 8W; $d\varepsilon/dt = 0.01\ s^{-1}$; $P_{relaxation}$ = 1 kPa; no wetting

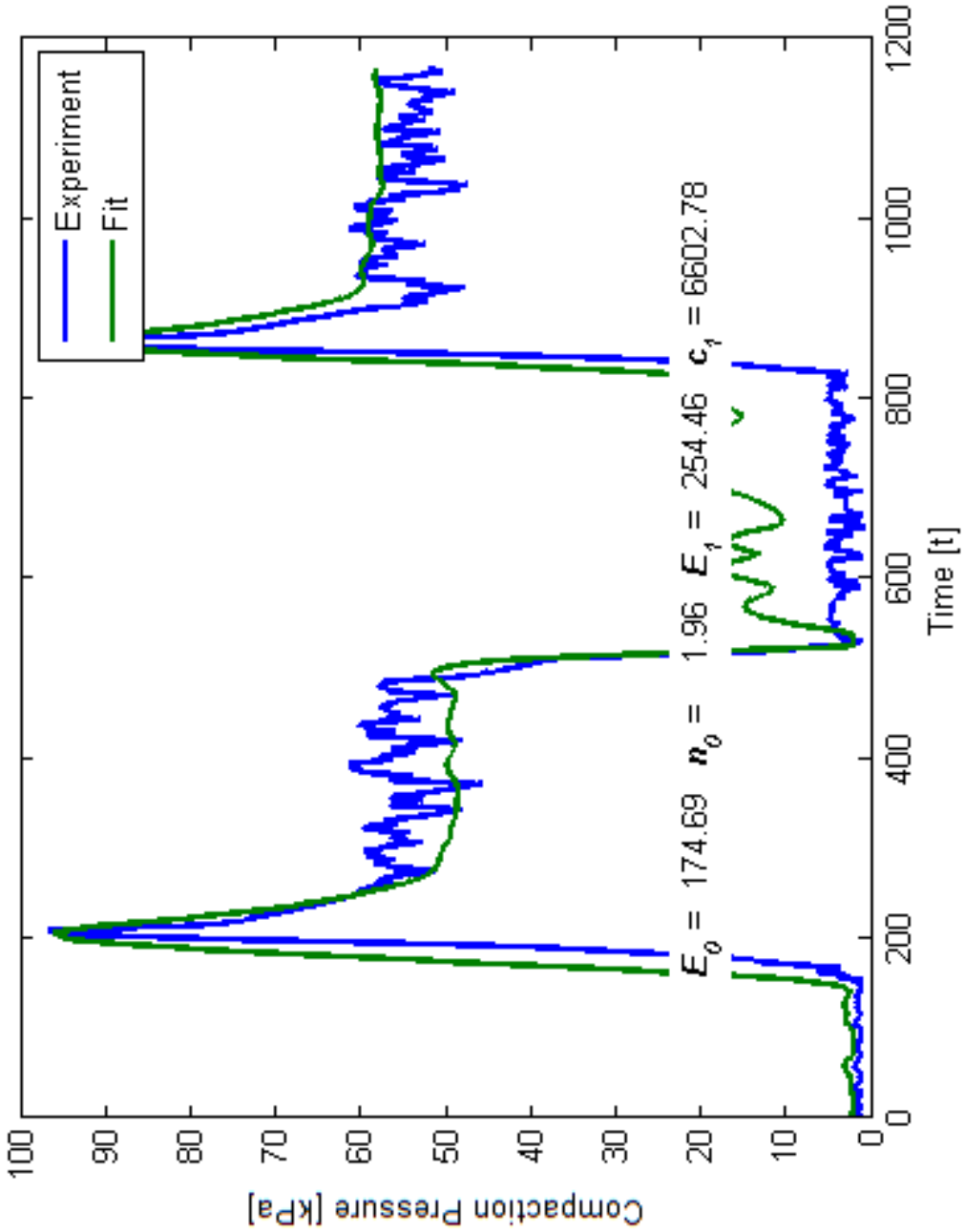

Figure 4.10. Model fits on experimental results for 8W; $d\mathcal{E}/dt = 0.01\ s^{-1}$; $P_{relaxation} = 1$ kPa

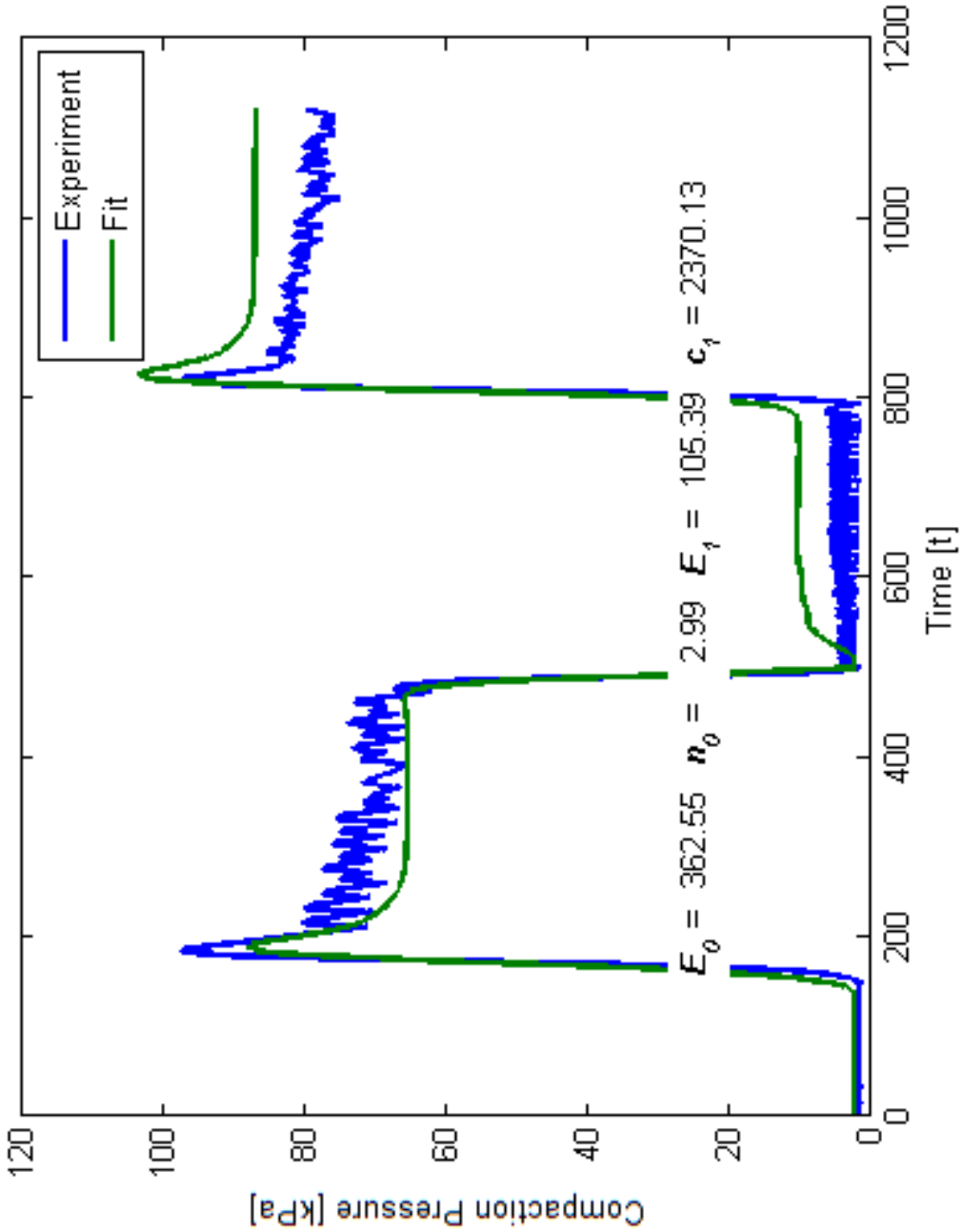

Figure 4.11. Model fits on experimental results for 8W; $d\varepsilon/dt = 0.02\ s^{-1}$; $P_{relaxation} = 1$ kPa

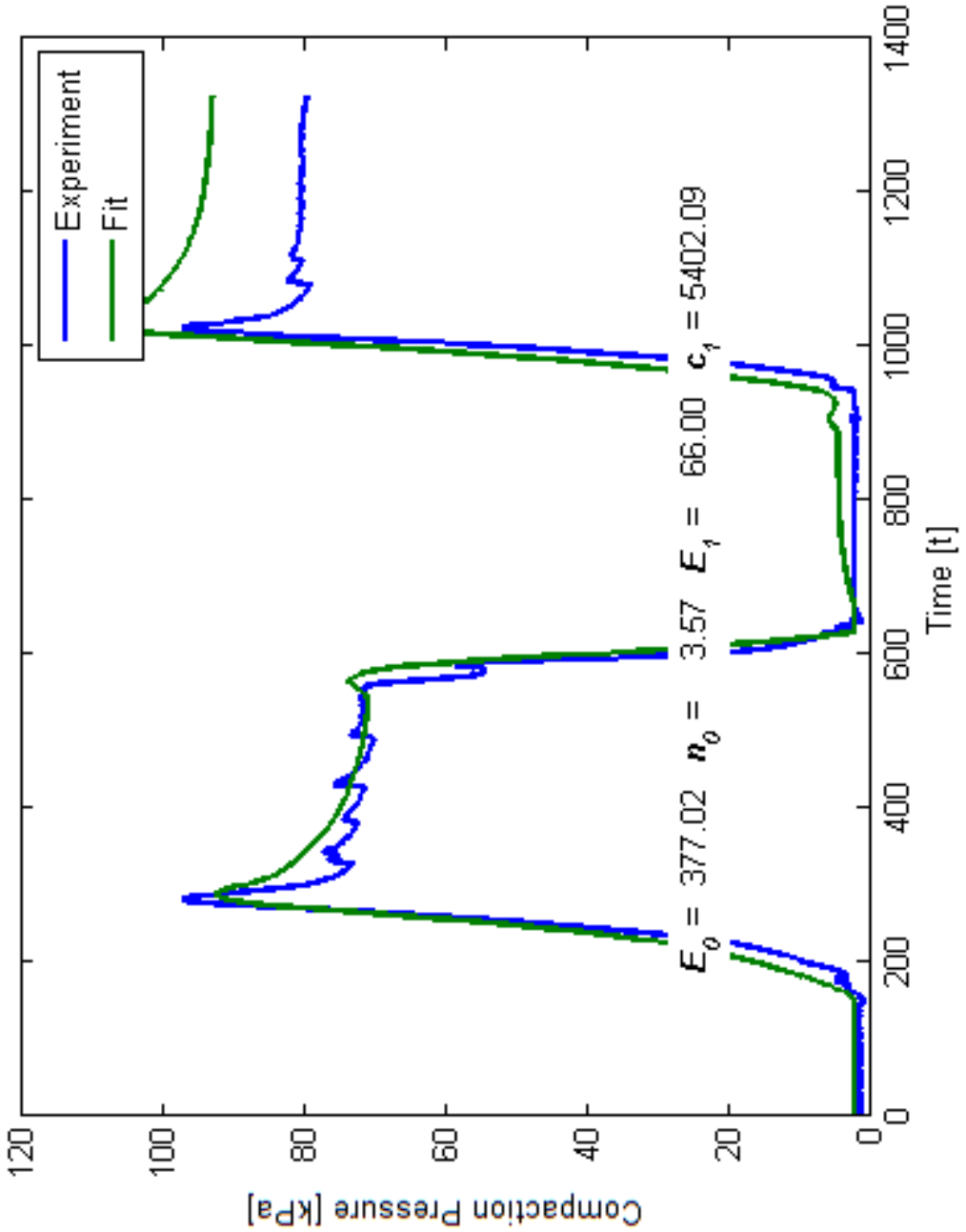

Figure 4.12. Model fits on experimental results for 8W; $d\varepsilon/dt = 0.005\ s^{-1}$; $P_{relaxation} = 1$ kPa

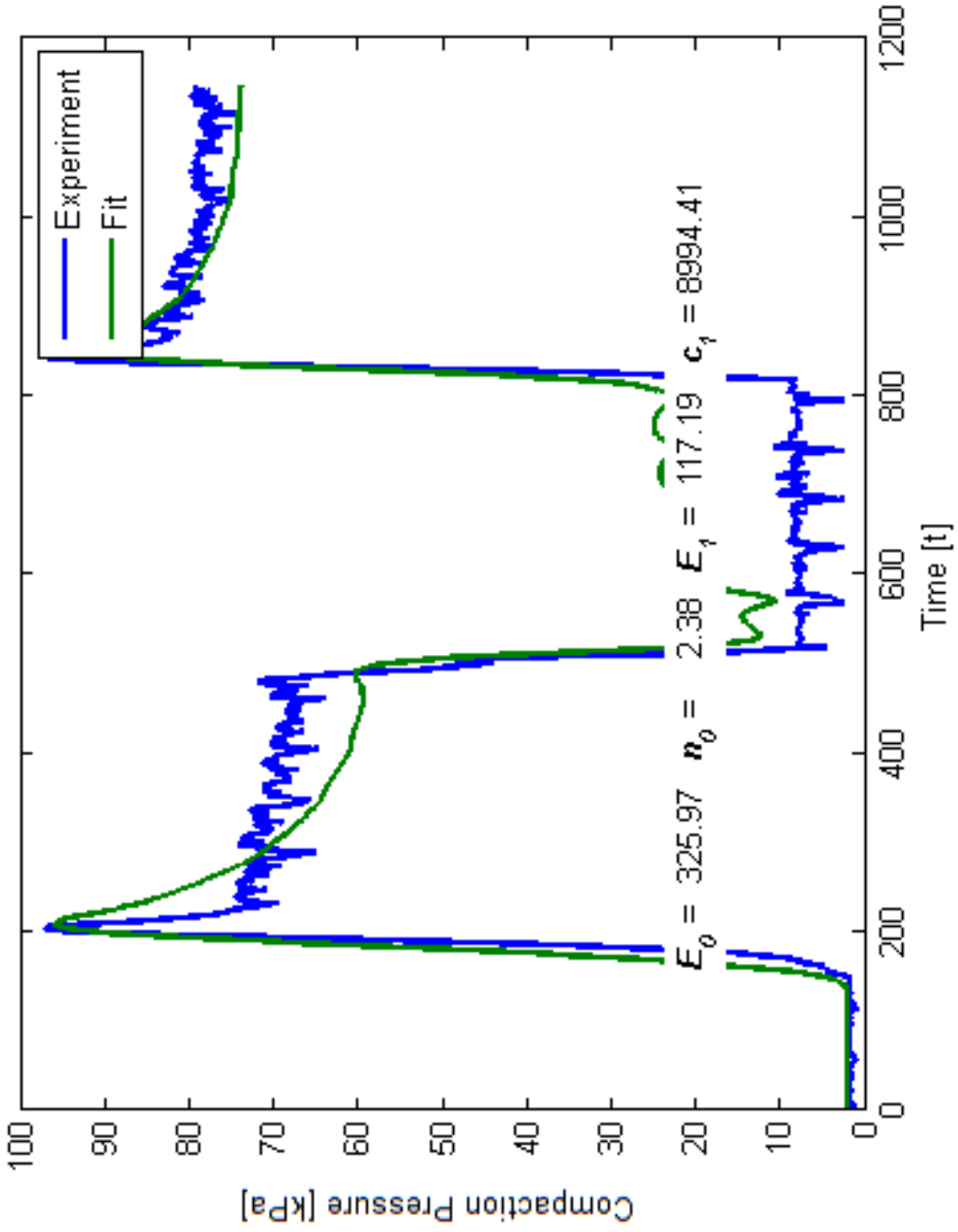

Figure 4.13. Model fits on experimental results for 8W; $d\varepsilon/dt = 0.01\ s^{-1}$; $P_{relaxation} = 5$ kPa

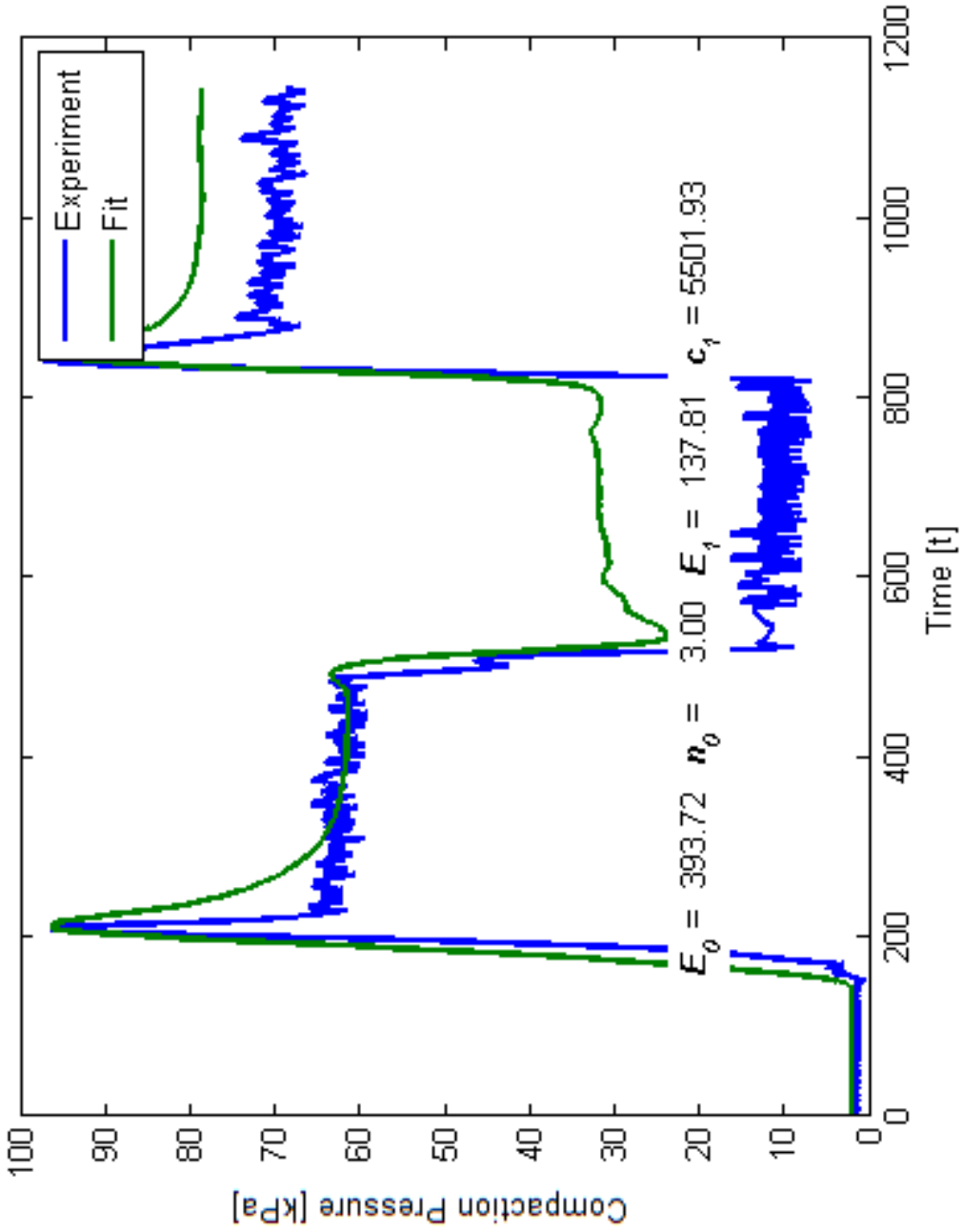

Figure 4.14. Model fits on experimental results for 8W; $d\varepsilon/dt = 0.01\ s^{-1}$; $P_{relaxation} = 10$ kPa

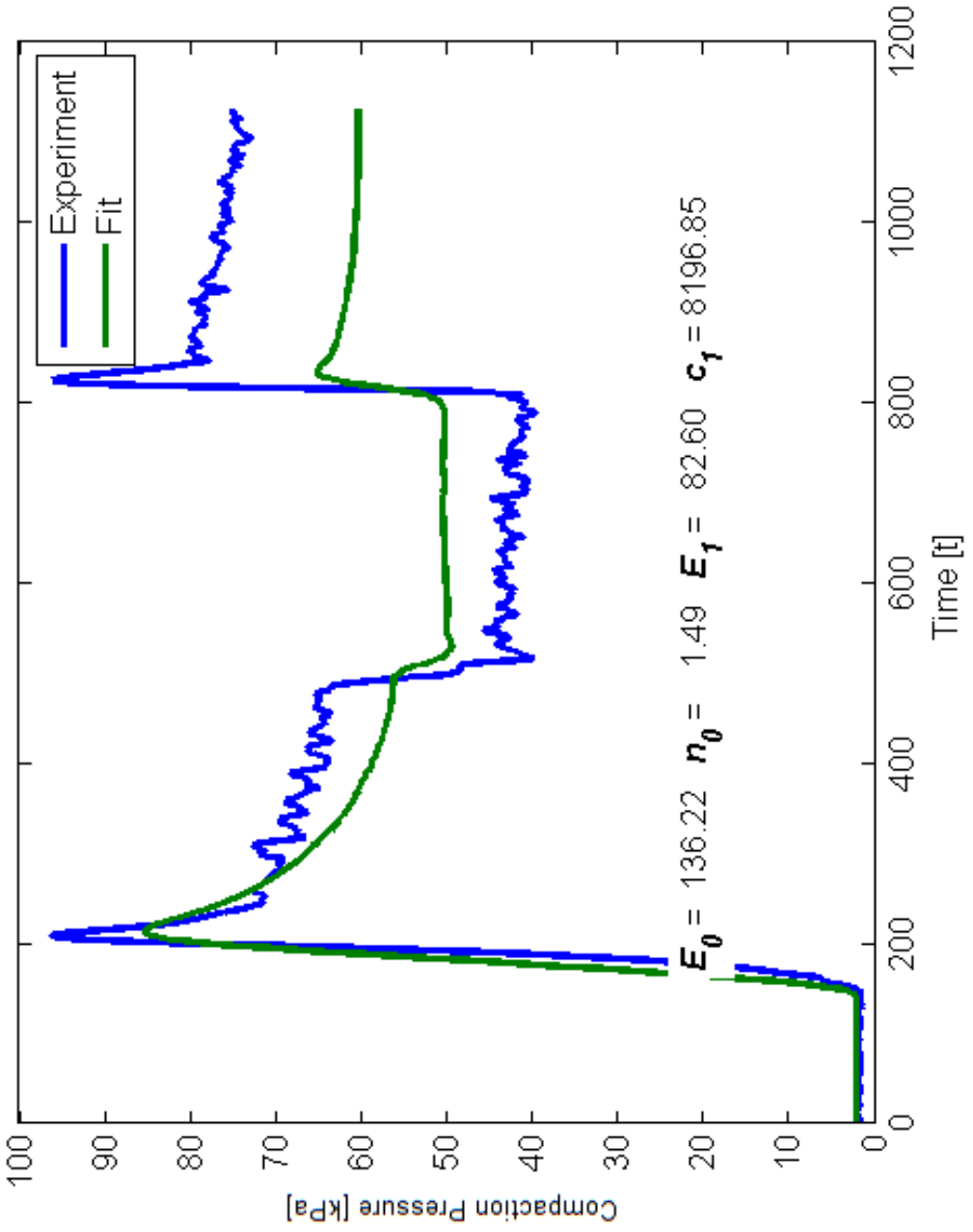

Figure 4.15. Model fits on experimental results for 8W; $d\mathcal{E}/dt = 0.01\ s^{-1}$; $P_{relaxation}$ = 40 kPa

There is a variation of compaction characterization for each experiment performed in this study meaning that the final thicknesses at major and minor compaction loads may be different. Therefore, the loading and unloading durations of each experiment may not be the same for all experiments in an experiment set because of the constant strain rates. For this reason, only one experiment for each set is used to fit the compaction model.

Chapter 5

SUMMARY AND CONCLUSION

A conventional Vacuum Infusion (VI) experimental setup integrated with a laser displacement measurement sensor and a PID controller was constructed to perform strain rate controlled material characterization experiments. Tuning of the PID constants (K_p, K_d and K_i) was investigated.

Strain rate controlled compaction and decompaction experiments were performed to characterize the compaction behaviors of two types of e-glass fabrics (random and woven). Various experimental procedures were designed by varying $d\varepsilon/dt$ (0.01 s^{-1} (nominal), 0.005 s^{-1} and 0.02 s^{-1}), $P_{relaxation}$ (1 kPa (nominal), 5 kPa, 10 kPa and 40 kPa) and wetting conditions (dry/dry and dry/wet (nominal) before and after the unloading stage). The compaction model adapted from Yenilmez's PhD thesis [4] was used to fit the experimental data with the model.

Just after P_c reached a peak value of 97.5 kPa, a stress relaxation was observed while keeping the strain constant at settling stages of all experiments. This behavior proved the presence of the viscous behavior in the compaction characterization of e-glass fabrics. Performing the characterization experiments at different $P_{relaxation}$ values allowed observing

the change in the viscoelastic behavior. In the experiments with low $P_{relaxation}$ values such as 1-10 kPa, P_c was reduced from 97.5 kPa to that particular value of 1-10 kPa with a constant strain rate; then the last strain was measured as $\varepsilon_{relaxation}$; and the strain was controlled with time to keep it at that particular value of $\varepsilon_{relaxation}$. It was observed that P_c slightly increased with time. However, this behavior was not observed at high P_c value of 40 kPa. During the relaxation stages of experiments at $P_{relaxation}$ = 40 kPa for both random and woven fabrics, the slight pressure increase was not observed. Therefore, one can conclude that the viscous behavior is not present for those experiments. As a matter of fact, in some of those experiments, a slight stress relaxation was observed (i.e., P_c slightly decreased with time) which leaded to the conclusion that the settling stage continued.

The fiber nesting due to wetting, which was indicated in Bayrak's MSc thesis [19] and [2], could not be observed clearly in strain rate controlled experiments performed in this study. To observe the nesting effect, the pressure rate controlled experiments can be performed which are conducted in Yenilmez's PhDd thesis [4].

The comparison of the two types of characterization experiments (pressure rate and strain rate controlled) and an investigation of the model parameters for both experiments are continued in Yenilmez's PhD thesis [4].

BIBLIOGRAPHY

[1] Yenilmez B, Senan M, Sozer EM. Variation of part thickness and compaction pressure in vacuum infusion process. Composites 2009; 69:1710-1719.

[2] Yenilmez B, Sozer EM. Compaction of e-glass fabric preforms in the vacuum infusion Process, A: Characterization experiments. Composites: Part A 2009; 40:499-510.

[3] Kelly PA, Umer R, Bickerton S. Viscoelastic response of dry and wet fibrous materials during infusion processes. Composites: Part A 2006; 37:868-873.

[4] Yenilmez B. Vacuum infusion (VI) process modeling and material characterization with viscoelastic compaction models. Ph.D. Thesis, Koc University, Graduate School of Engineering, 2012.

[5] Akyol T. Minimizing thickness variation in the vacuum infusion (VI) process with 1D and 2D resin flows. M.Sc. Thesis, Koc University, Graduate School of Engineering, 2012.

[6] Saunders RA, Lekakou C, Bader MG. Compression in the processing of polymer composites 1. A mechanical and microstructural study for different glass fabrics and resins. Composites Science and Technology 1999; 59:983-993.

[7] Chen B, Lang EJ, Chou T-W. Experimental and theoretical studies of fabric compaction behaviour in resin transfer moulding. Materials Science and Engineering 2001; A317:188–196.

[8] Bickerton S, Buntain MJ, Somashekar AA. The viscoelastic compression behavior of liquid composite molding preforms. Composites: Part A 2003; 34: 431-444.

[9] Govignon Q, Bickerton S, Kelly PA. Simulation of the reinforcement compaction and resin flow during the complete resin infusion process. Composites: Part A 2010; 41:45-57.

[10] Yuexin D, Zhaoyuan T, Yan Z, Jing S. Compression responses of preform in vacuum infusion process. Chinese Journal Of Aeronautics 2008; 21:370-377.

[11] Saunders RA, Lekakou C, Bader MG. Compression in the processing of polymer composites 2. Modelling of the viscoelastic compression of resin-impregnated fibre networks. Composites Science and Technology 1999; 59:1483-1494.

[12] Hammami A. Effect of reinforcement structure on compaction behavior in the vacuum infusion process. Polymer Composites 2001; 22:337-348.

[13] Somashekar AA, Bickerton S, Bhattacharyya D. Exploring the non-elastic compression deformation of dry glass fibre reinforcements. Composite Science and Technology 2006; 67:183-200.

[14] Luo Y, Verpoest I. Compressibility and relaxation of a new sandwich textile preform for liquid composite molding. Polymer Composites 1999; 20(2):179-191.

[15] Chen B, Cheng AH-D, Chou T-W. A nonlinear compaction model for fibrous preforms. Composites: Part A 2001; 32:701-707.

[16] Visioli A. Tuning of PID controllers with fuzzy logic. IEEE Proc.-Control Theory Appl. 2001; 148(1):1-8.

[17] Ang KH, Chong G, Li Y. PID control system analysis, design, and technology. IEEE Transactions On Control Systems Technology. 2005; 13(4):559-576.

[18] Barret JF, Coales JF. An introduction to the analysis of non-linear control systems with random inputs. IEEE. 1955; 154:621-652.

[19] Bayrak T. Compaction experiments on different e-glass fabric preforms in the vacuum infusion process. M.Sc. Thesis, Koc University, Graduate School of Engineering, 2008.

VITA

Mustafa Reşit Haboğlu was born in Çorum, Turkey on February 10, 1987. He received his B. Sc. Degree in Mechatronics Engineering from Sabanci University, Istanbul, 2009. Since then, he has enrolled in the M. Sc. Program in Mechanical Engineering at Koc University, Istanbul as both a teaching and research assistant. His most recent thesis, "Strain rate controlled compaction characterization of e-glass fabrics and investigation of the effects of process parameters on the results" acts as a complement to his other VARTM related works. He is planning to continue his career as a PhD student in a university in Istanbul or a mechanical engineer in the industry.